Markus Elsing

Tracking at the LHC (Part 2)

- LHC Tracking Detectors

Introduction: the LHC and the Experiments

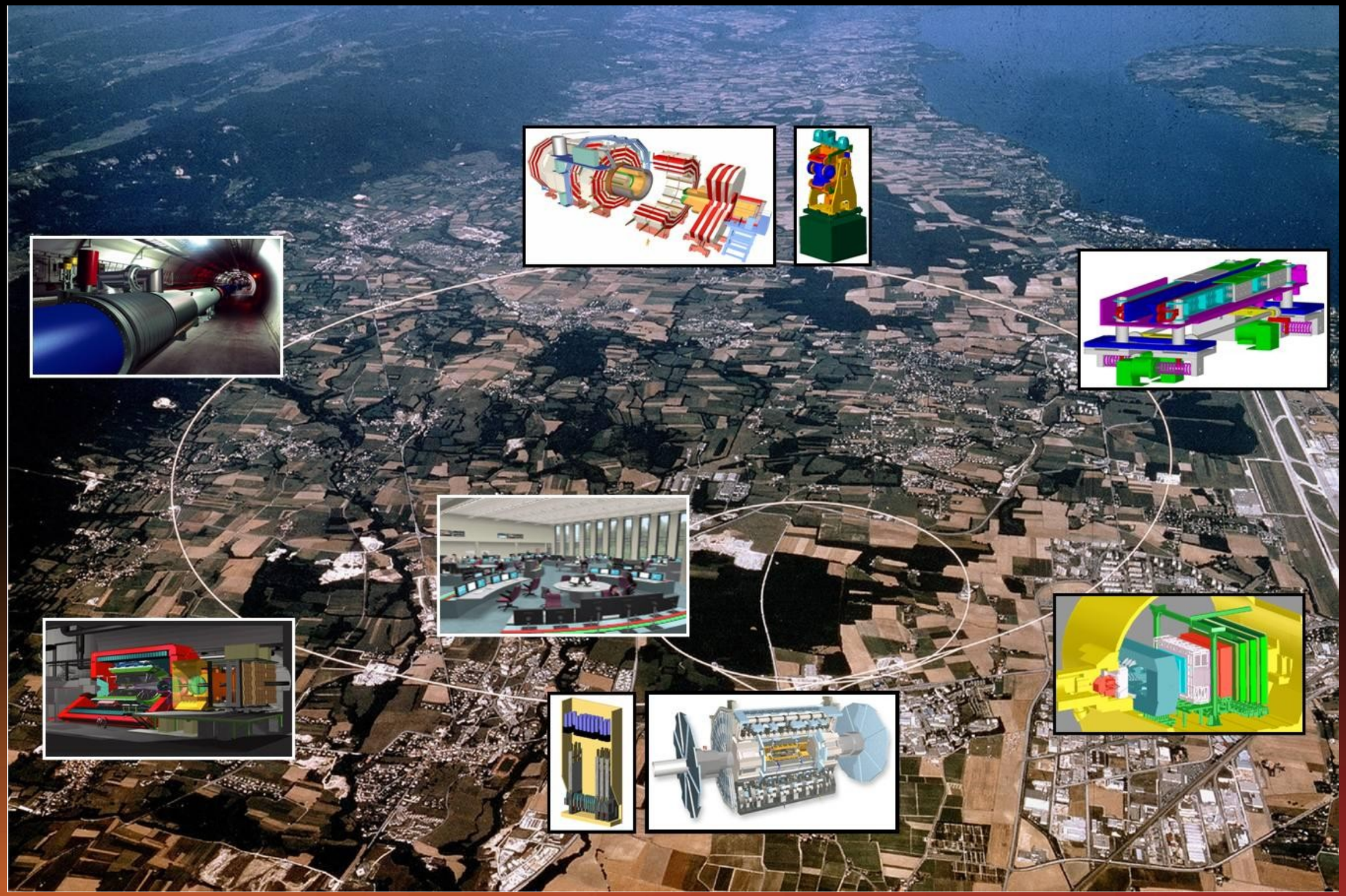

Introduction: the LHC and the Experiments

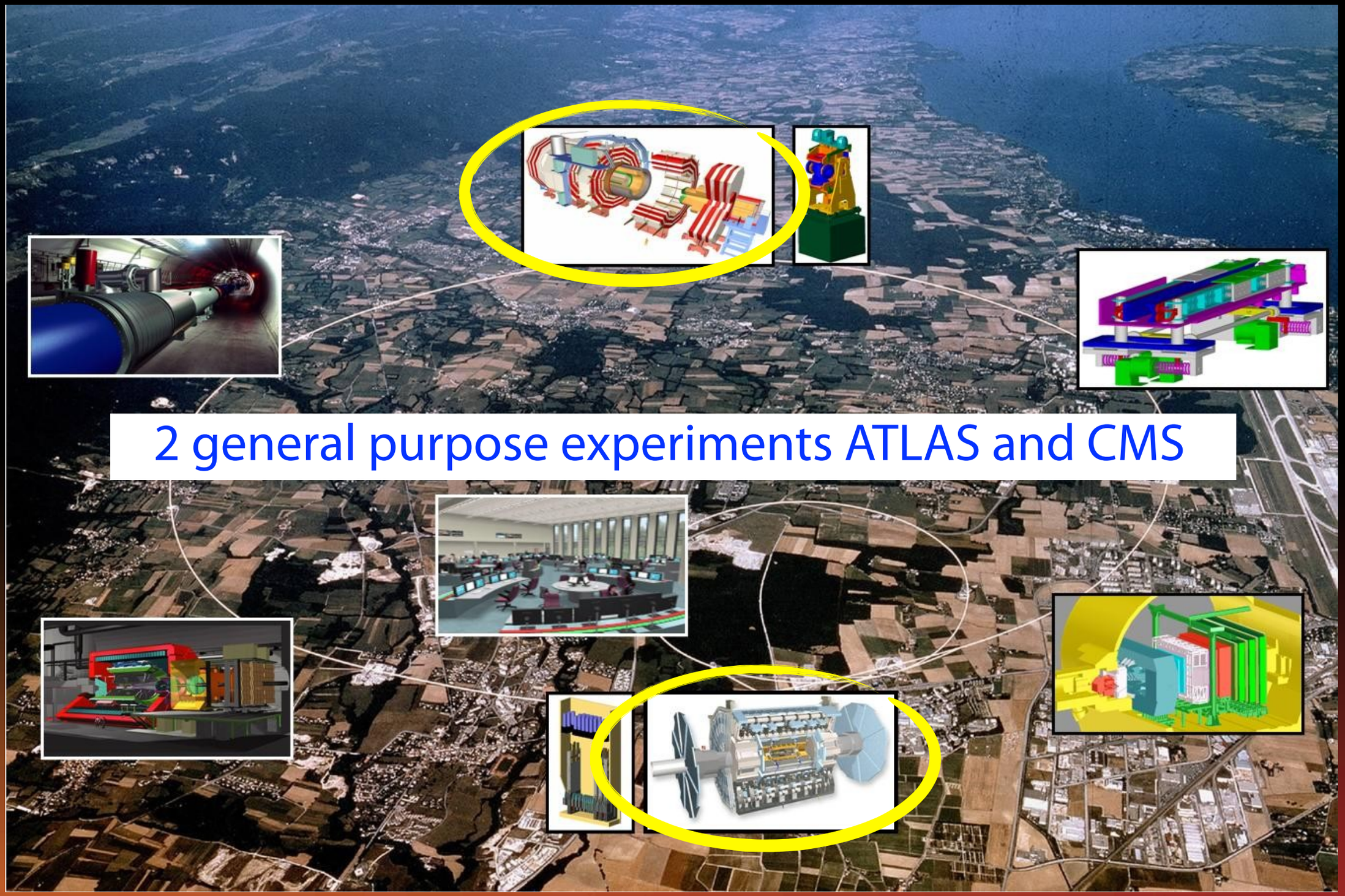

Introduction: the LHC and the Experiments

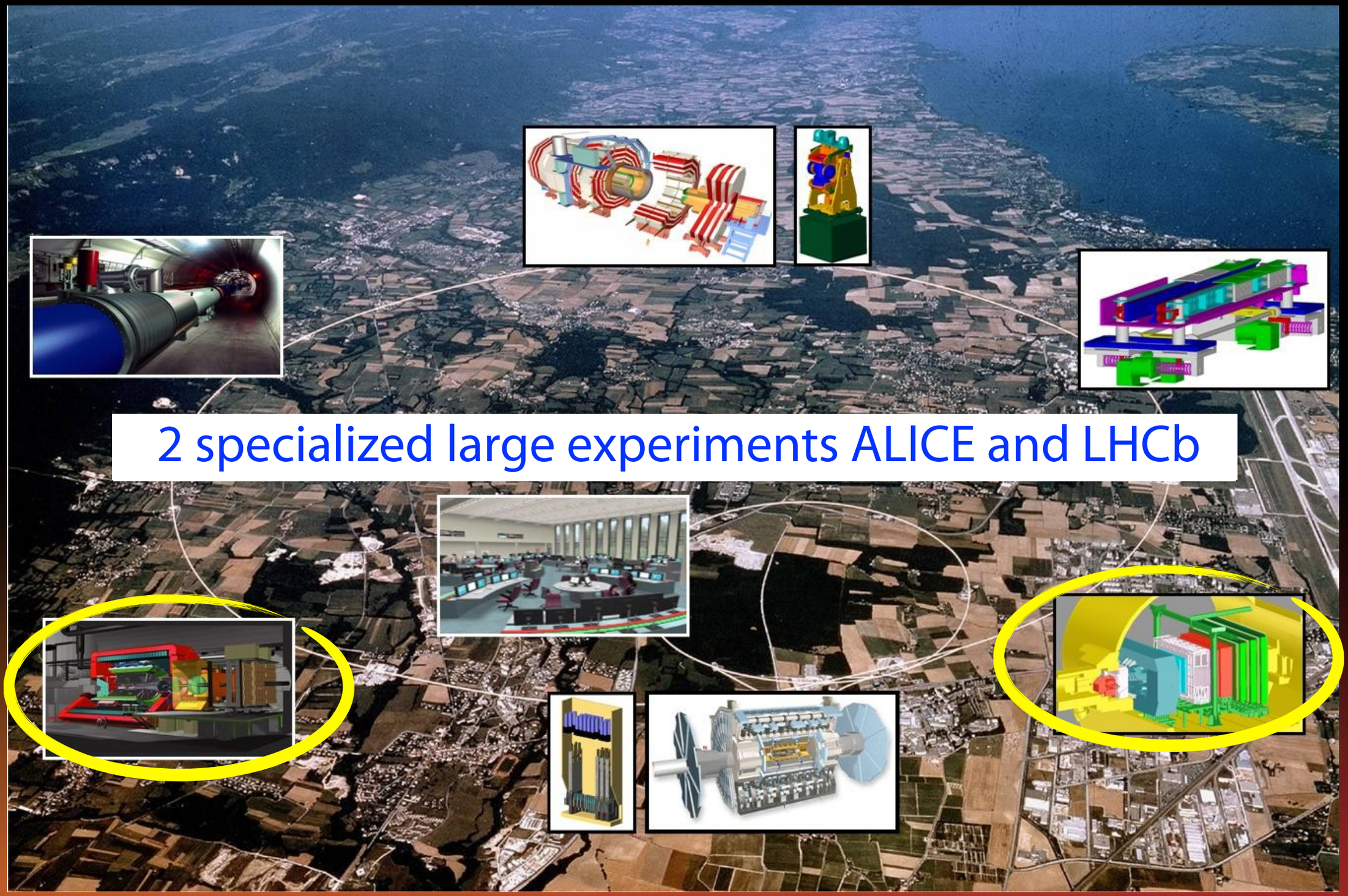

2 specialized large experiments ALICE and LHCb

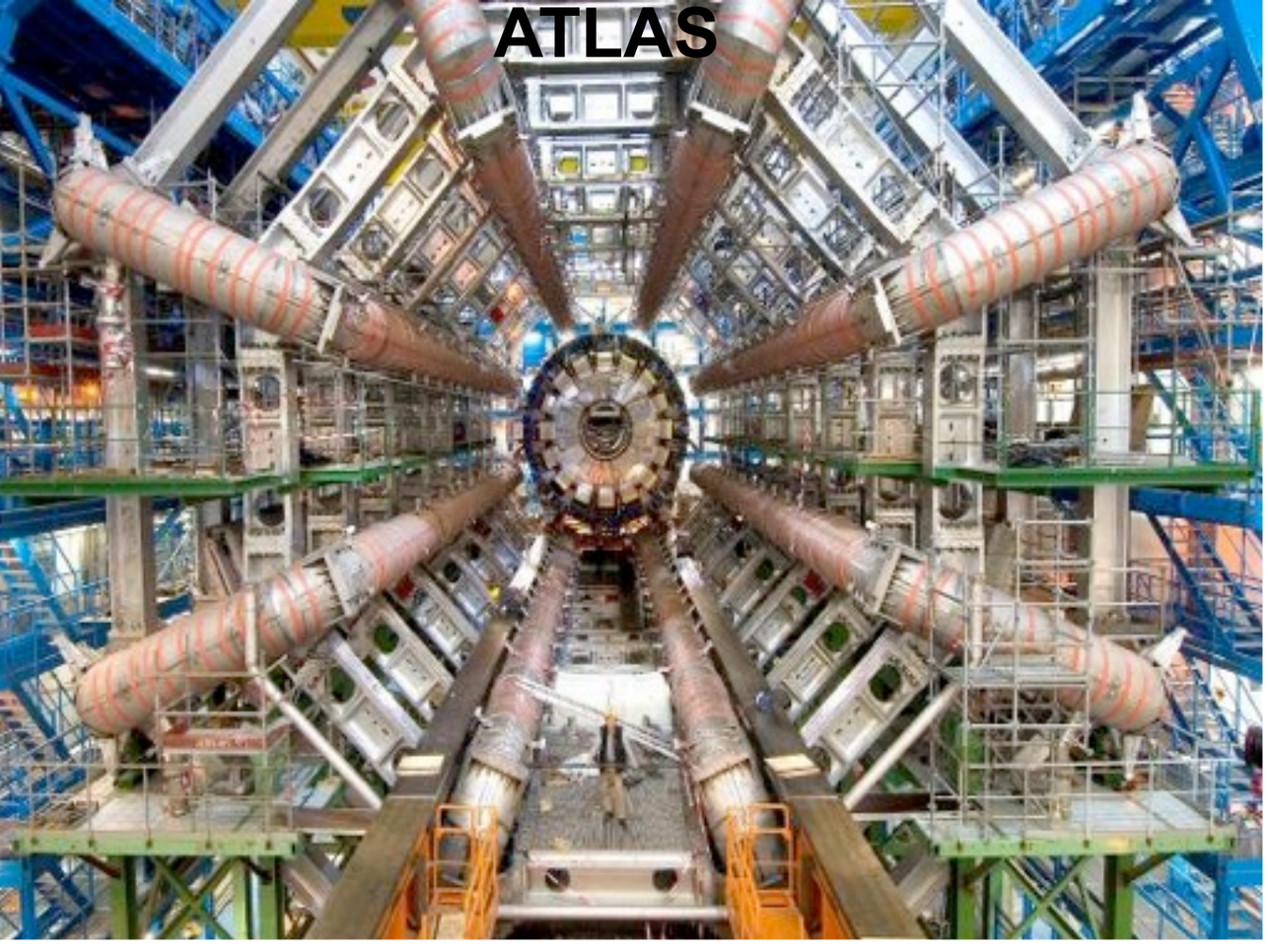
ATLAS

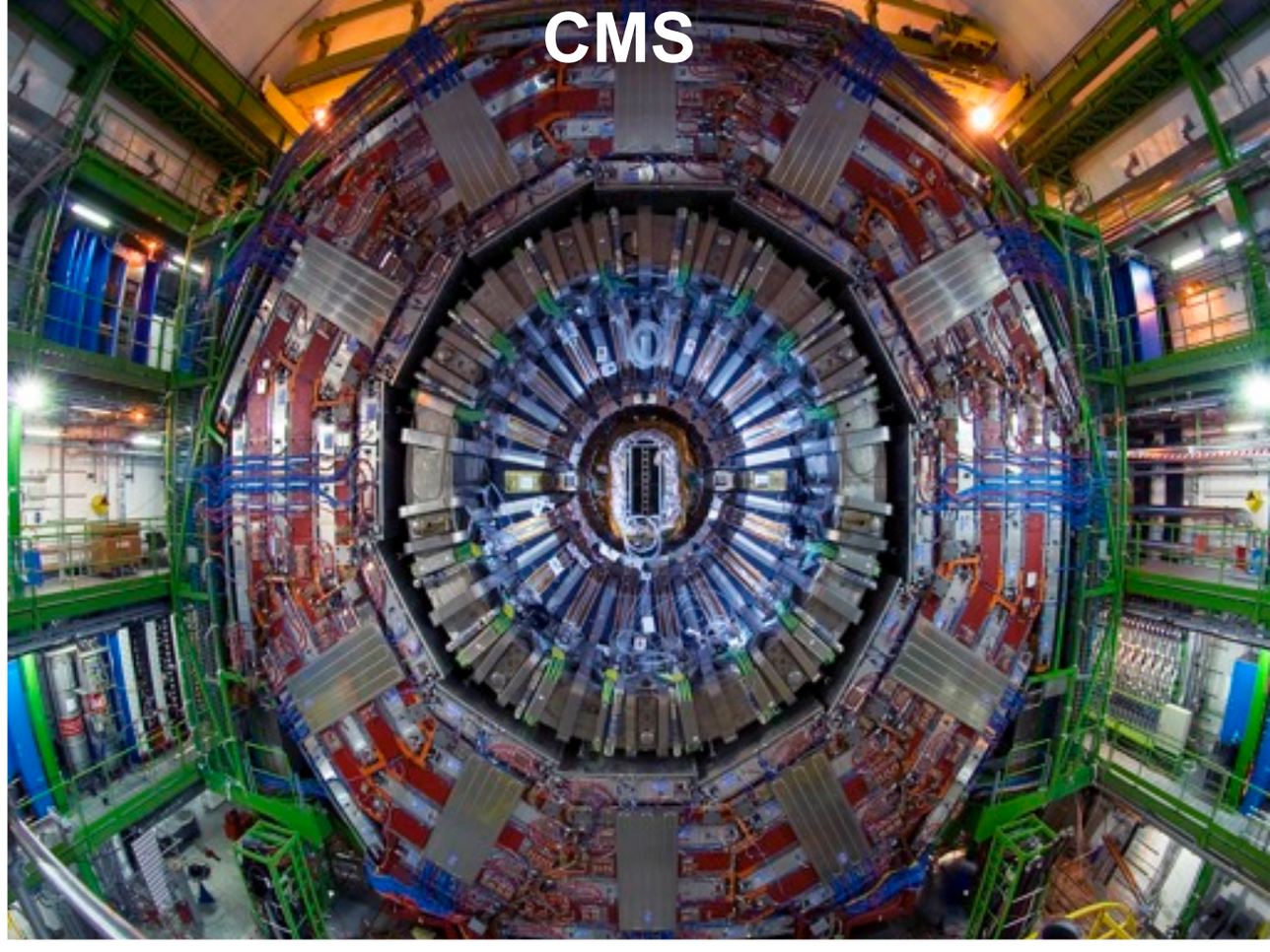
CMS


LHCb

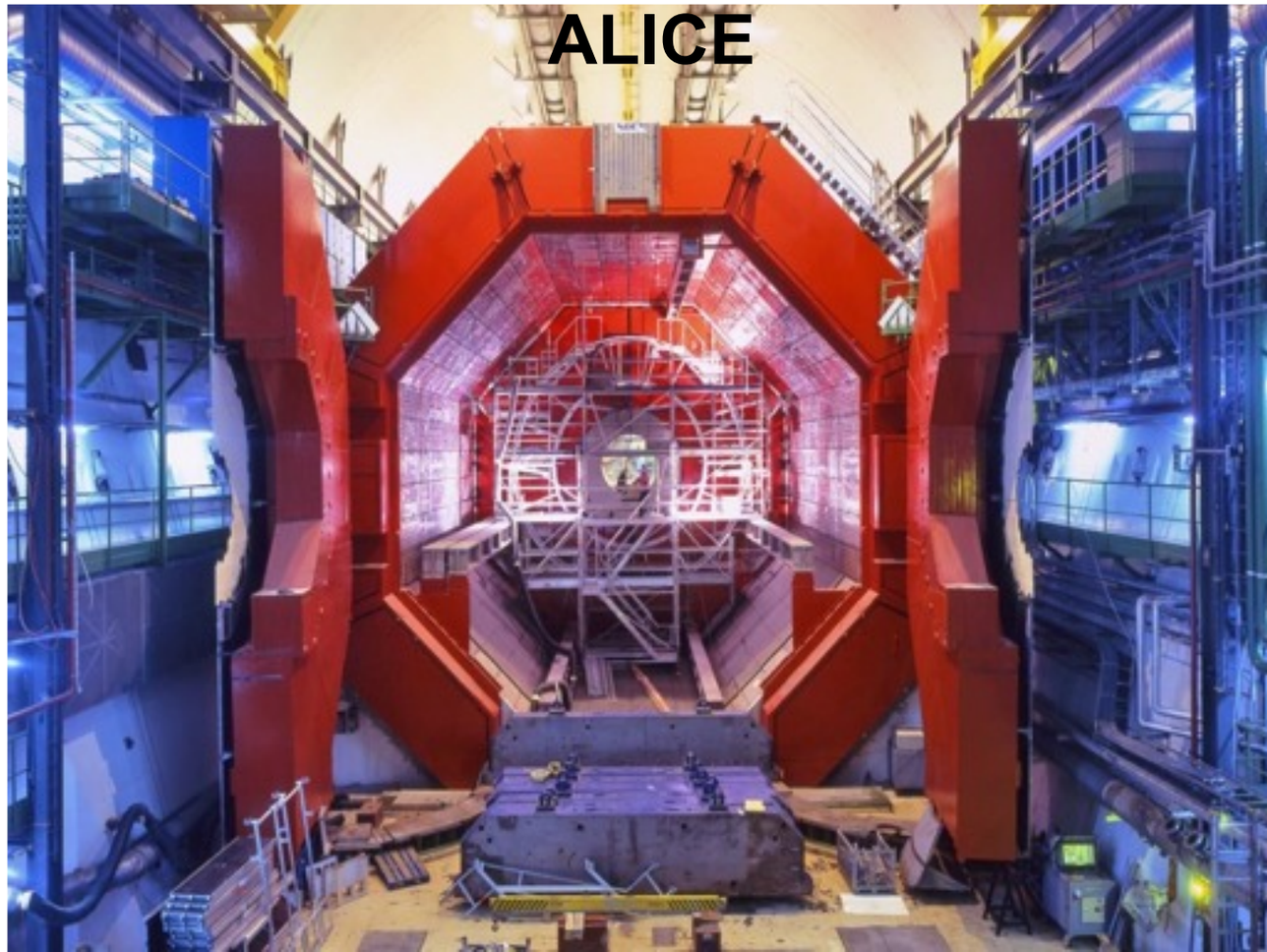
ALICE

Outline of Part 2

- give an overview of the LHC detectors
  - ➡ inner tracking and as well some words on the muon systems
- tracking detectors
  - ➡ discuss constraints, roles and design choices
- detector technologies and their applications
  - ➡ semiconductor trackers
  - ➡ drift tube detectors

ATLAS

- from the outside, all one sees are **muon chambers**
  - ➡ tracking of muons in toroid field

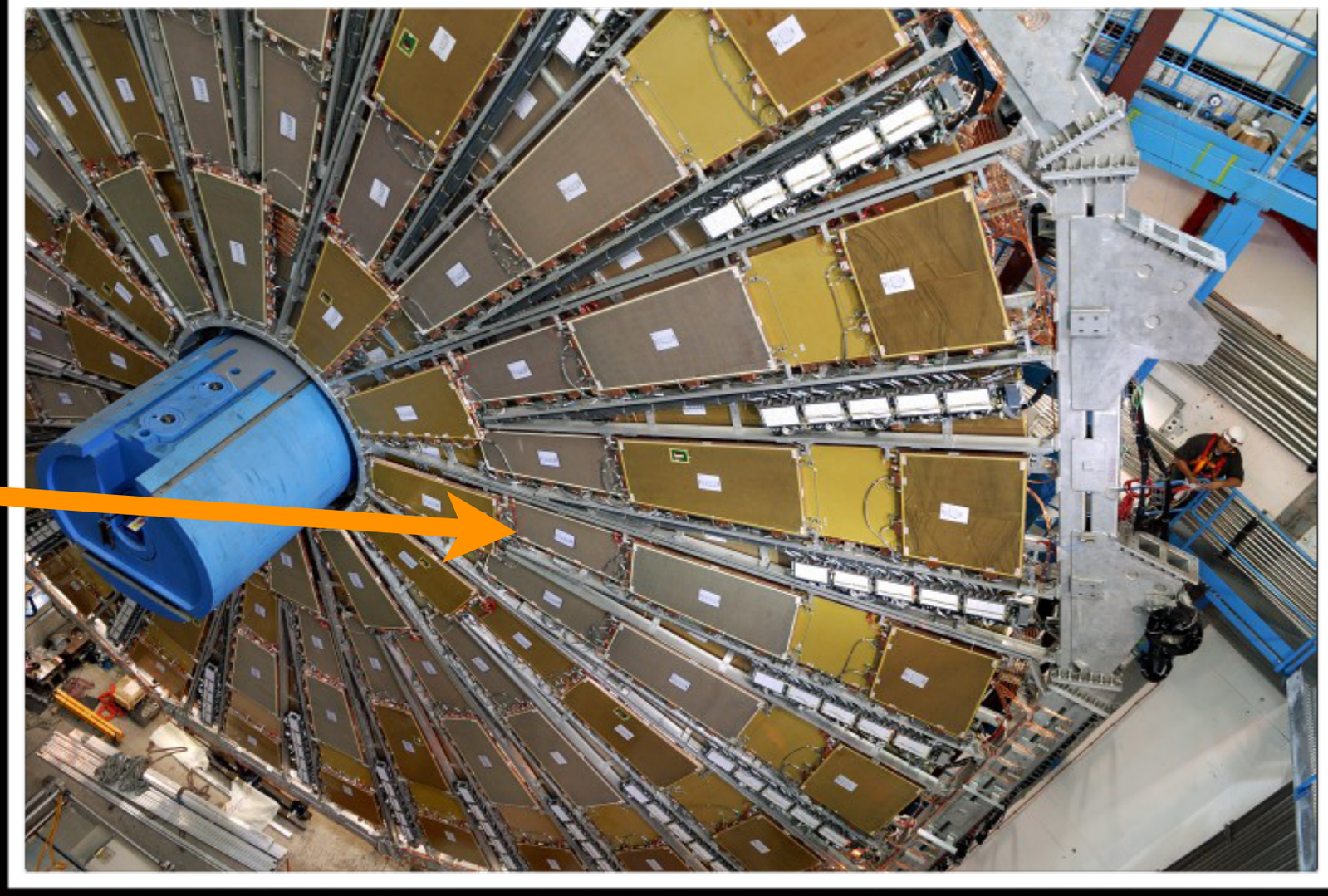

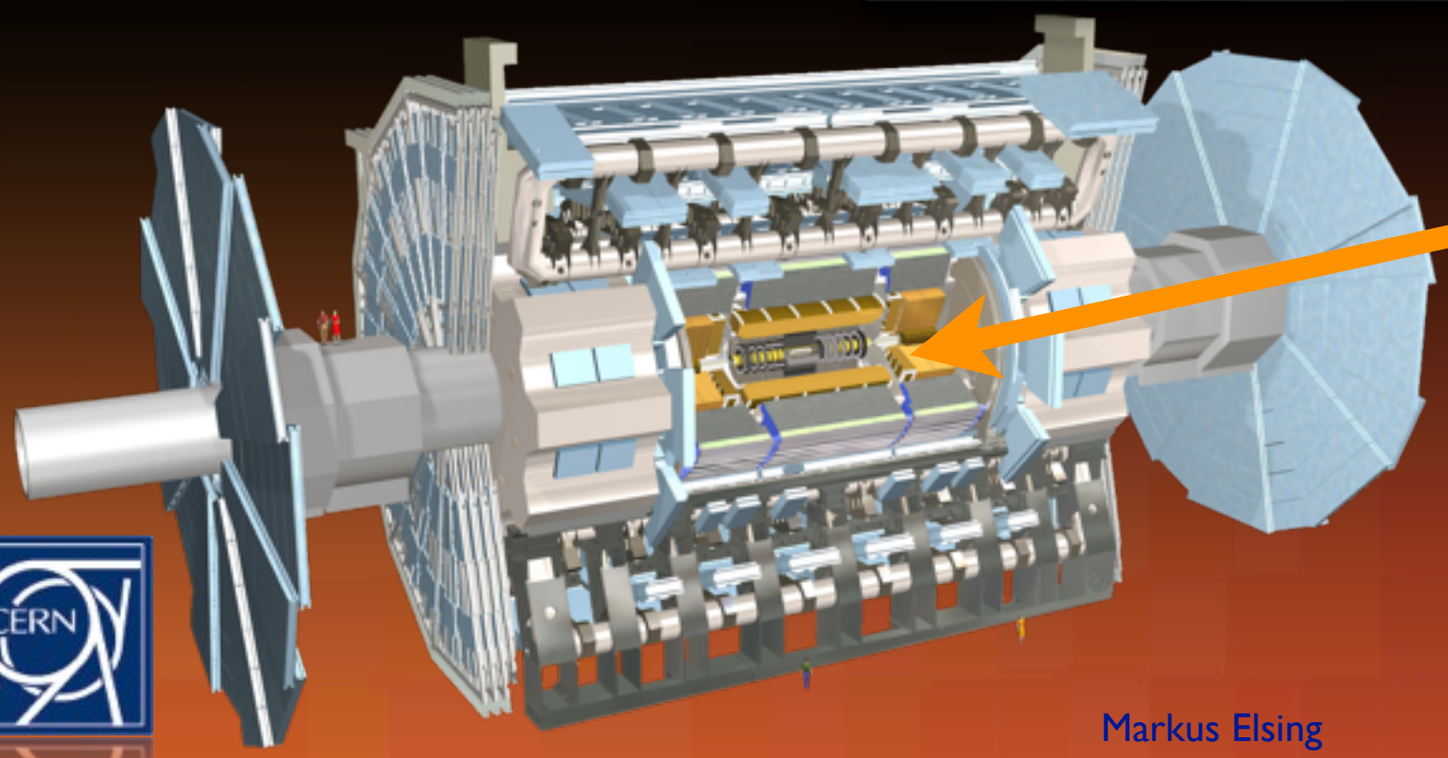

- ➡ most particles are absorbed in the **calorimeters**, which measure their energy
- ➡ not subject of these lectures

ATLAS

- from the outside, all one sees are **muon chambers**
  - ➡ tracking of muons in toroid field

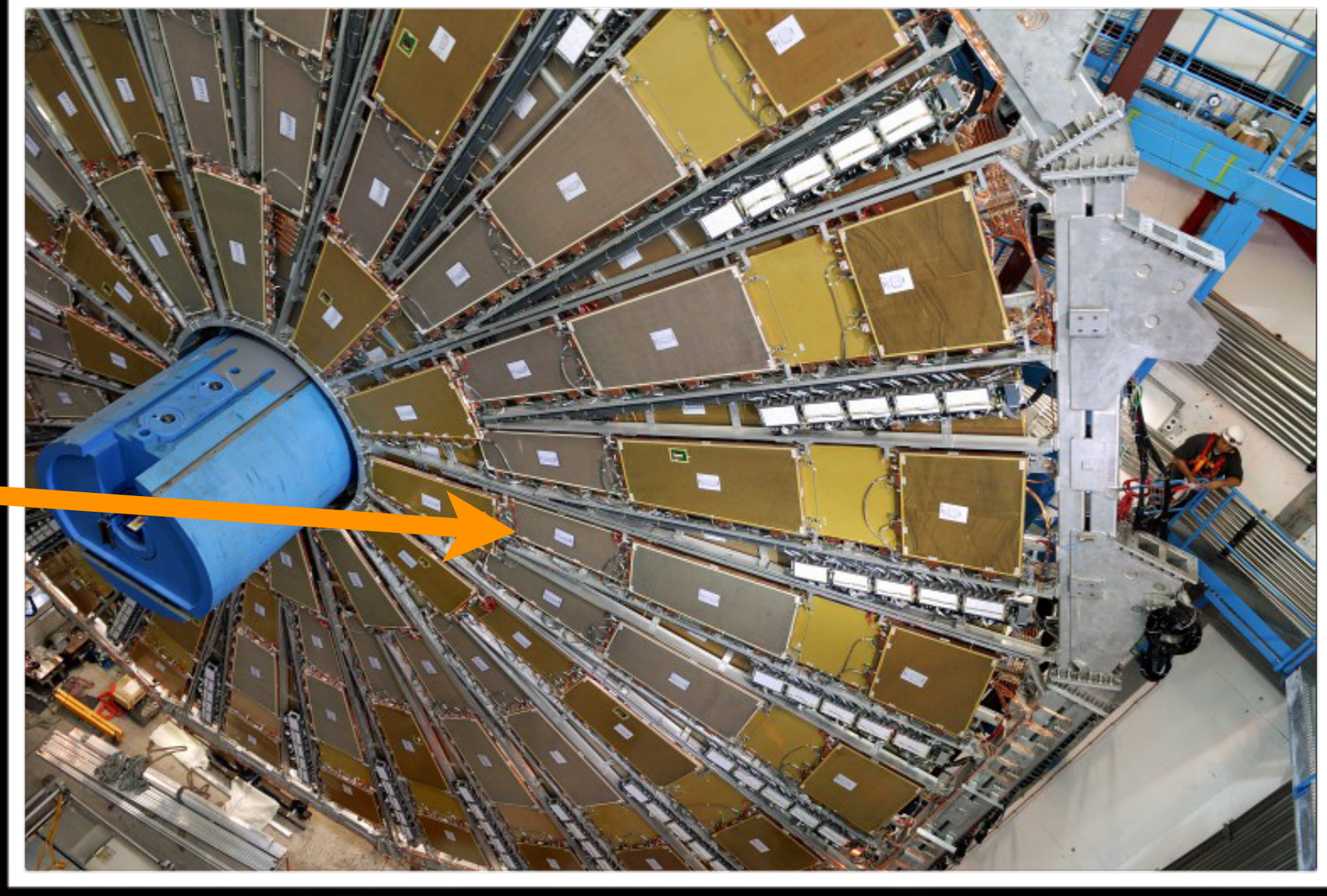

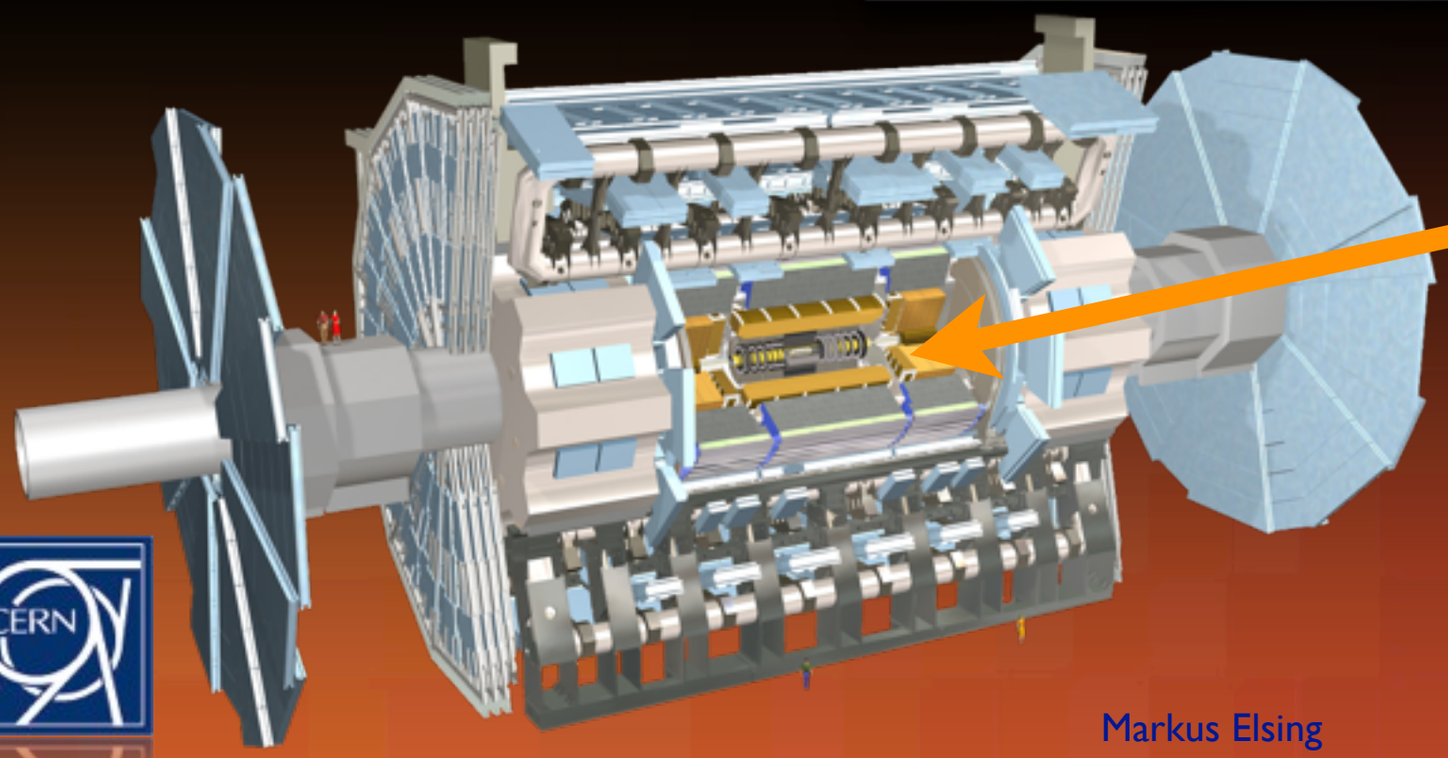

- ➡ most particles are absorbed in the **calorimeters**, which measure their energy
- ➡ not subject of these lectures

- let' have a brief look at the **muon systems**
  - ➡ ATLAS and CMS

ATLAS Muon Spectrometer

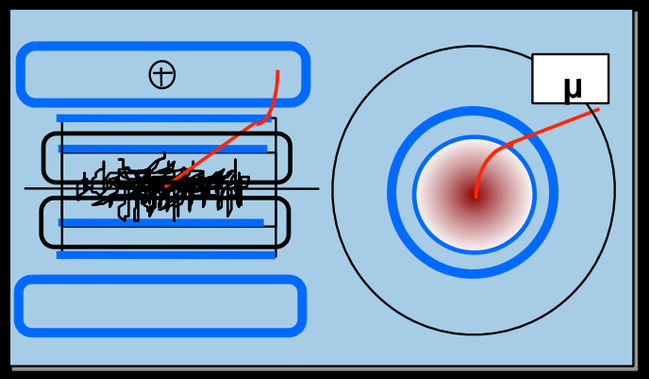

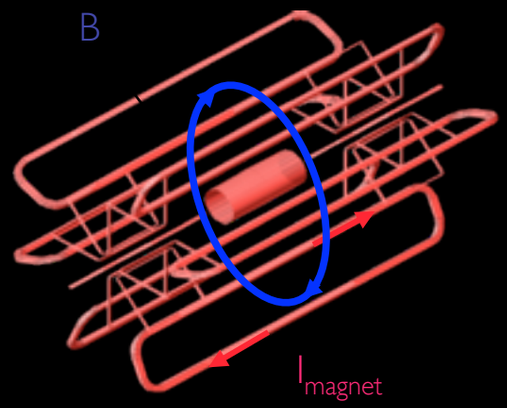

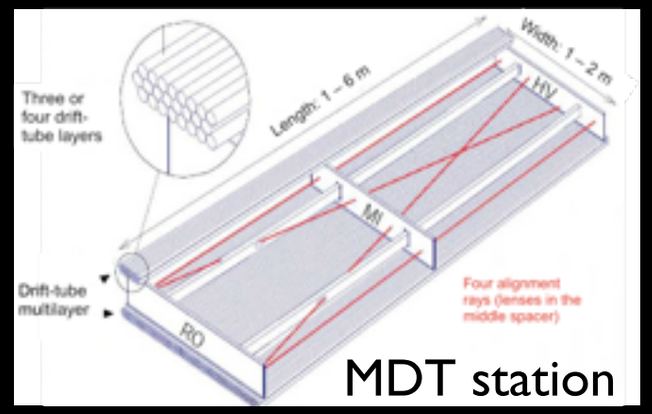

- a huge system
  - ➡ 4 different technologies (MDT,CSC,RPC,TGC)
  - ➡ large area (10.000 m²)
  - ➡ many channels (1 M)
- toroid field configuration
  - ➡ large magnetic field variations in toroid
  - ➡ field 4 Tesla near coils
- optical alignment system

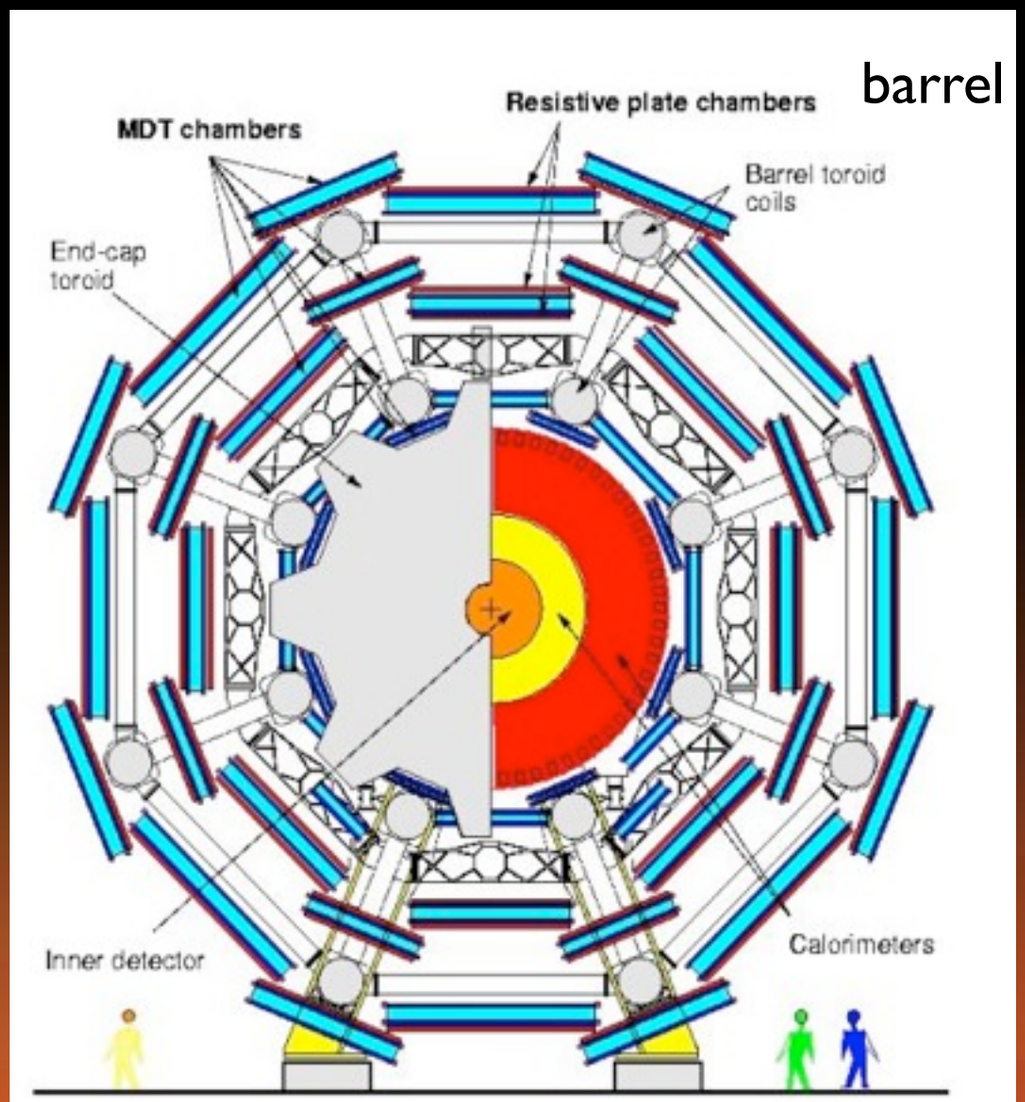

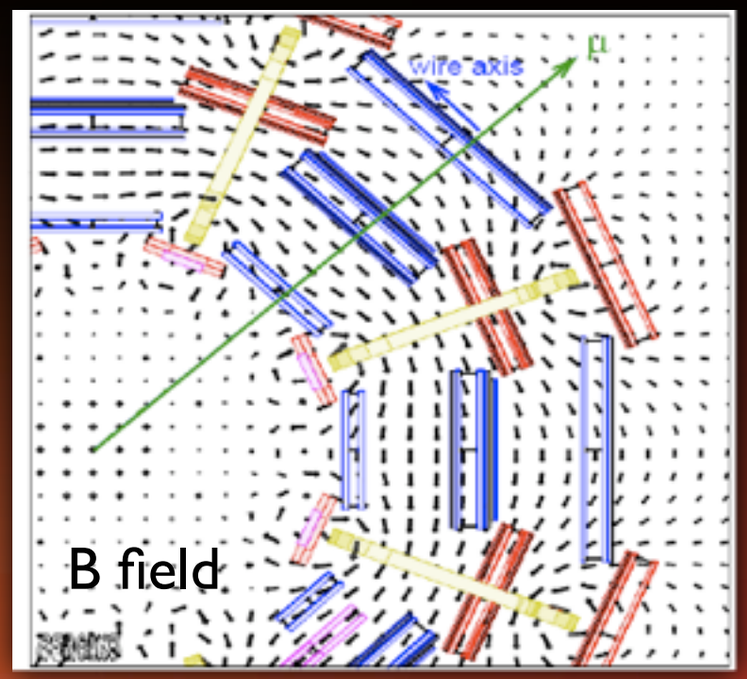

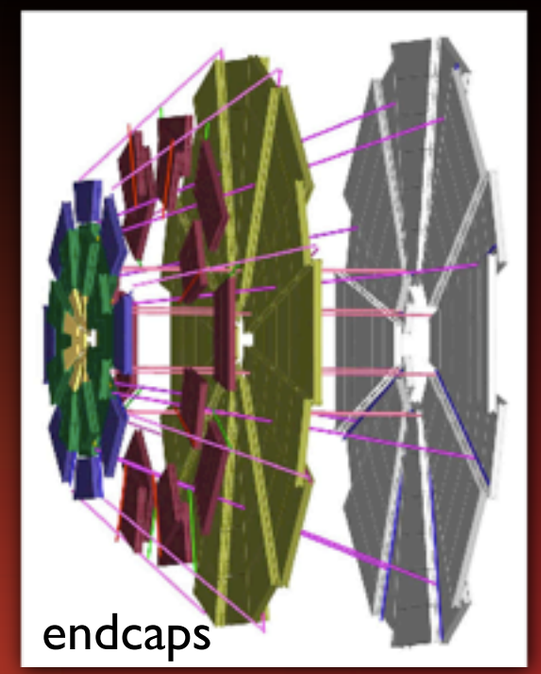

CMS Muon System

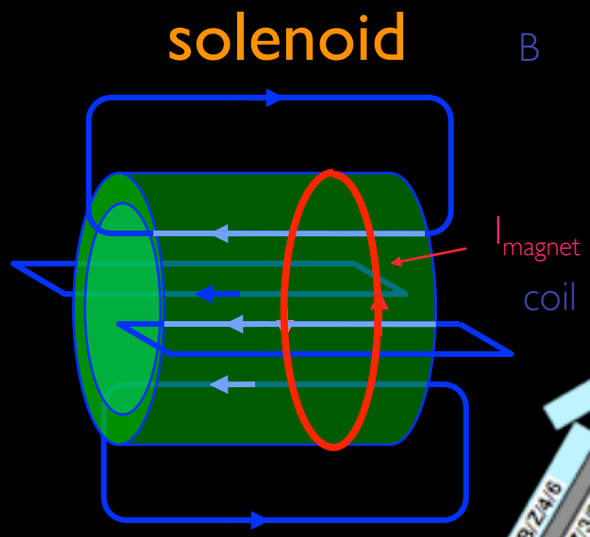

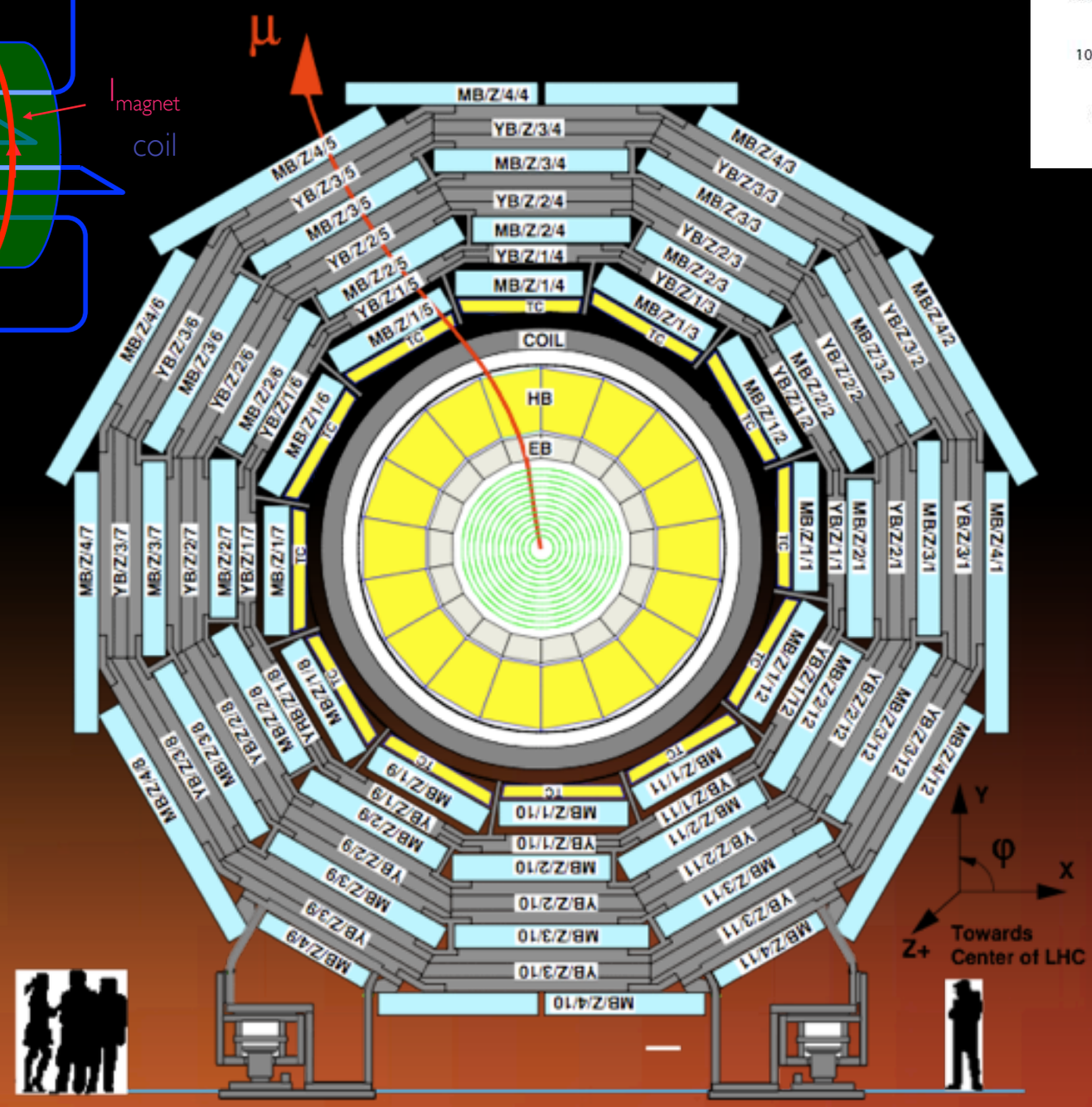

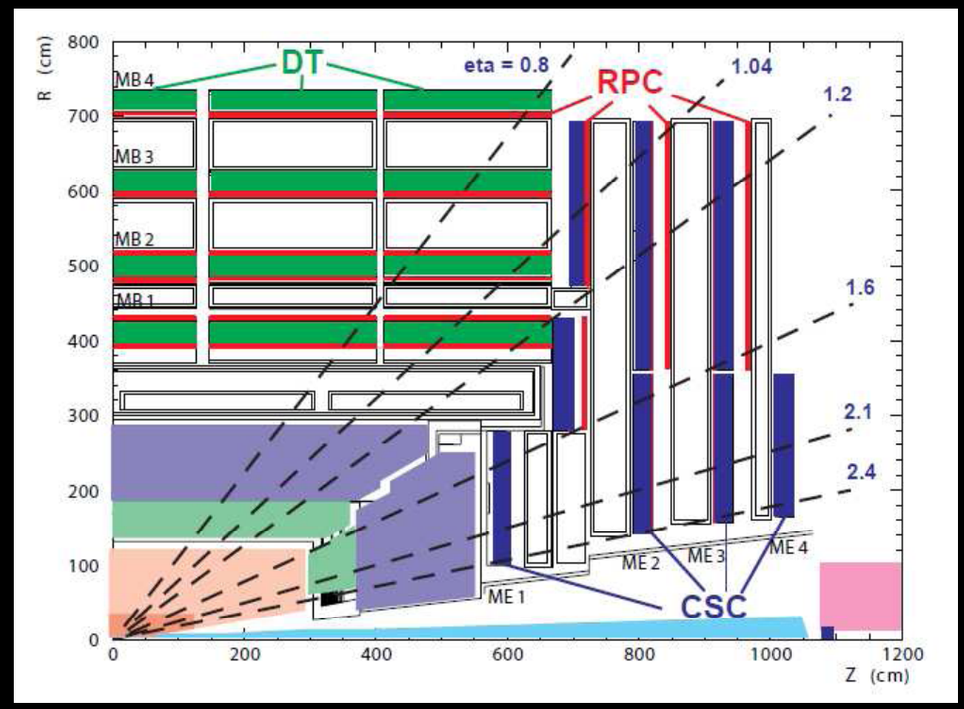

- Muon Drift Tubes
  - ➡ magnetic field return in iron yoke of solenoid
  - ➡ combine with precise p_T measurement in Tracker
- Cathode Strip Chambers
  - ➡ in the endcaps
- Resistive Plate Chambers

Expected Momentum Resolution

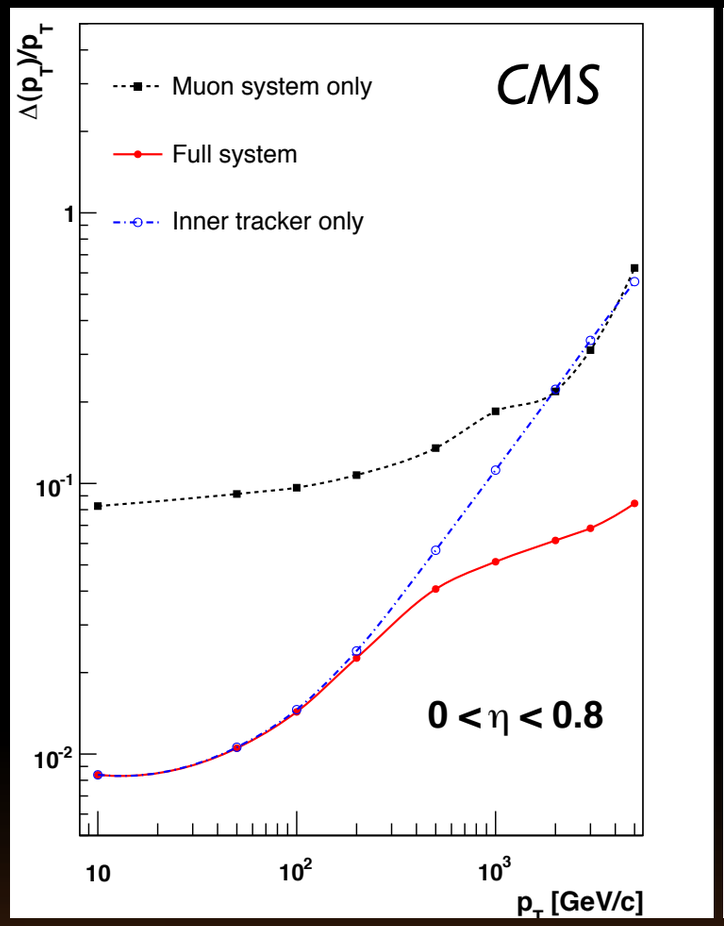

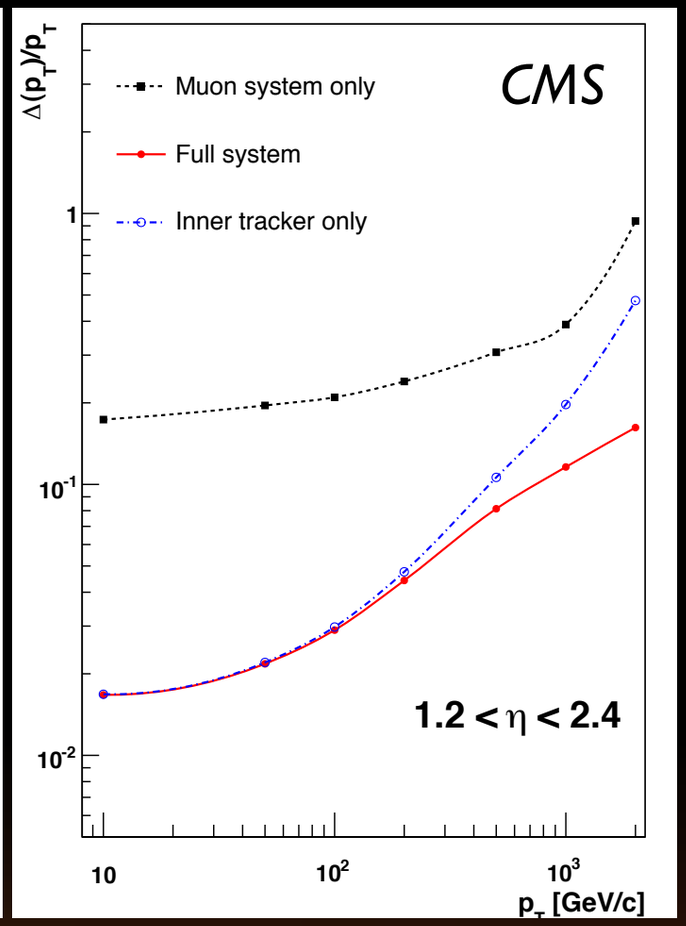

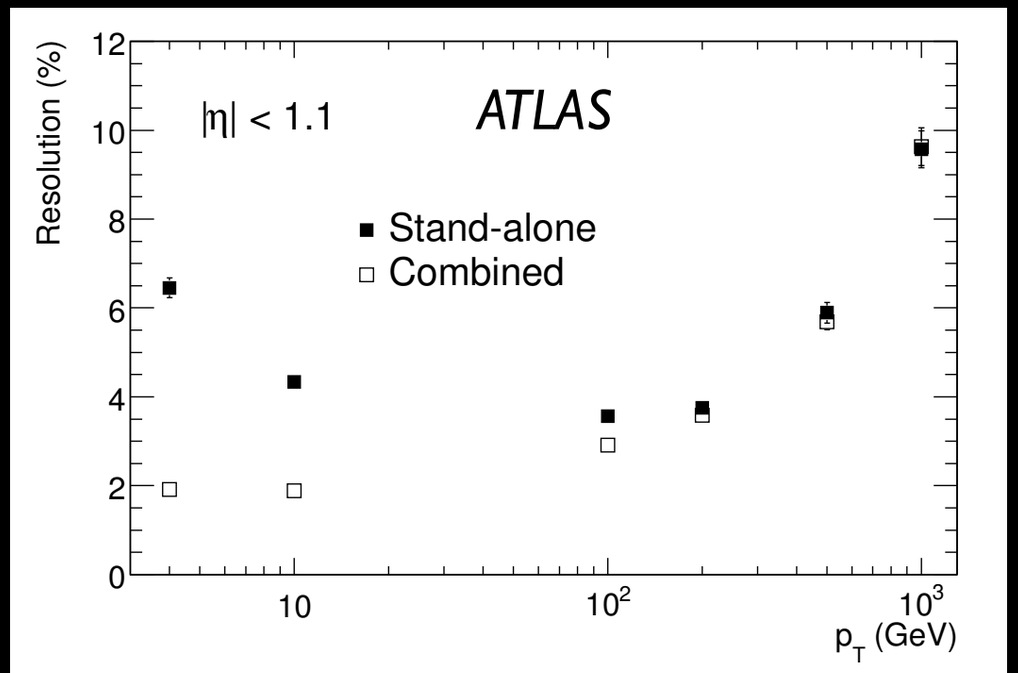

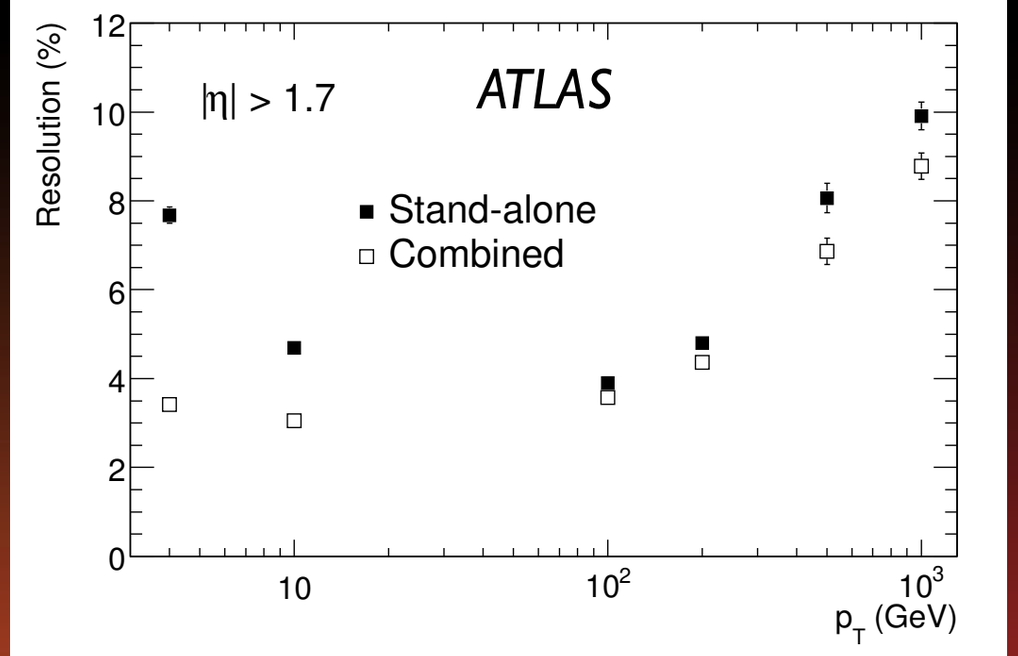

- comparable performance
  - ➡ CMS benefits from good Inner Tracker resolution
  - ➡ in ATLAS Muon Spectrometer dominates at high p_T
  - ➡ ATLAS has slightly larger η coverage

CMS

- in the following will concentrate on the central trackers

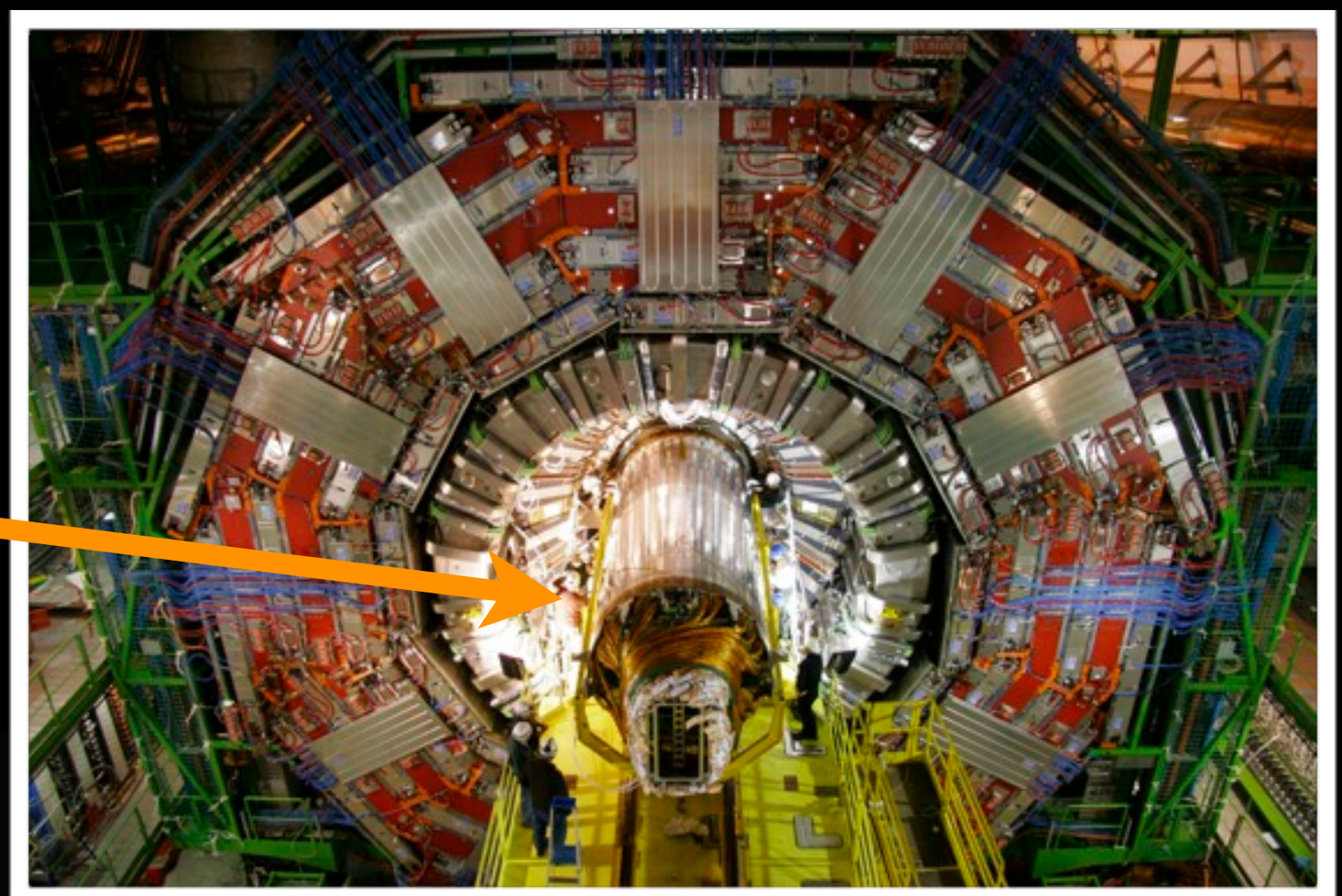

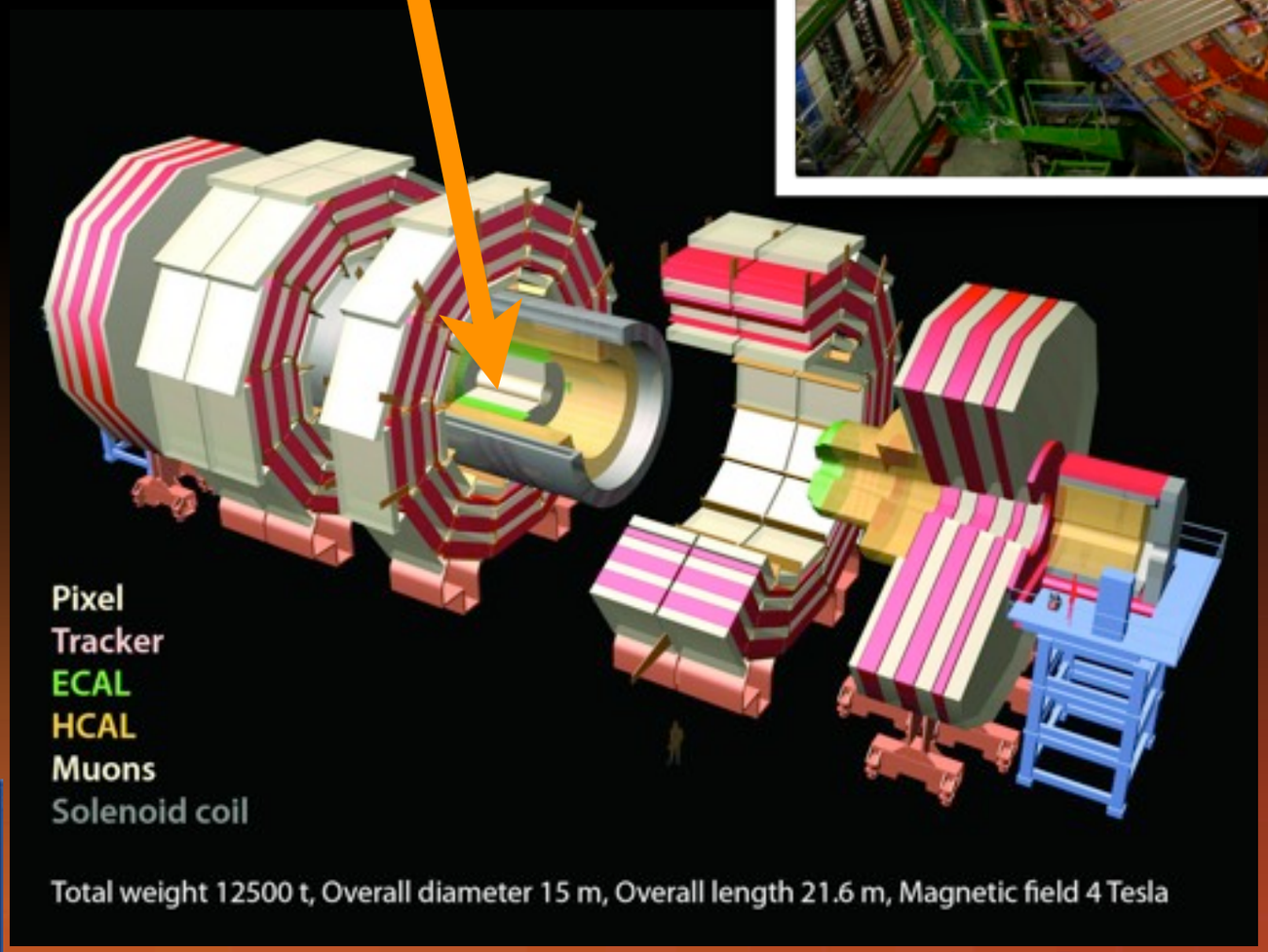

CMS

- in the following will concentrate on the central trackers

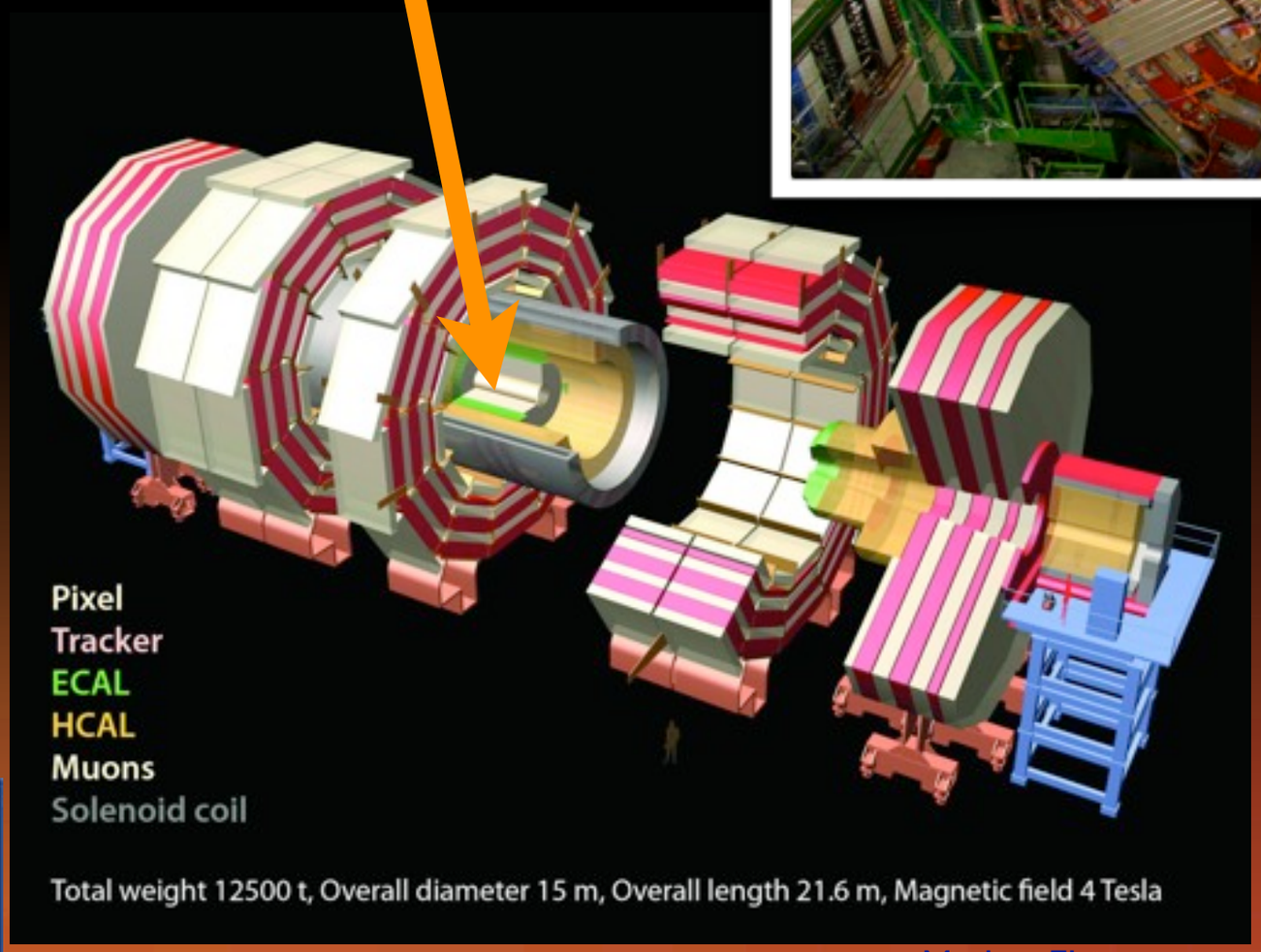

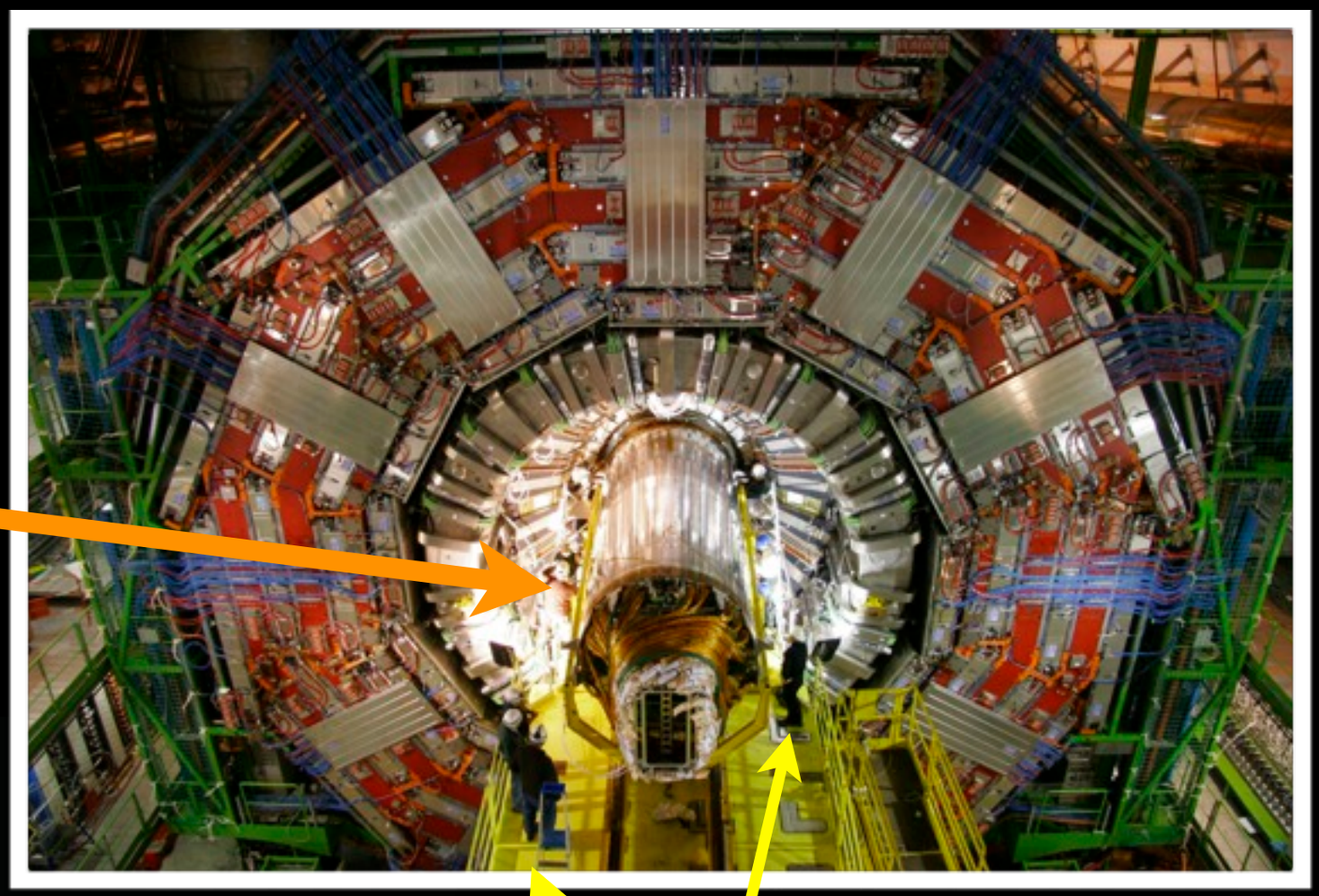

...like for sure they did as well

Constraints on Tracking Detectors

- high occupancy, high radiation dose, high data rate
  - ➡ at full design luminosity more than **20 interactions** per pp bunch crossing
    - more than a **1000 charged particles** in tracker, every 25ns.
  - ➡ even higher multiplicity in **central Pb-Pb collisions**
    - with >10000 charged particles in trackers
  - ➡ design for **10^{15} neq** (neutron equivalent) for innermost layers (10 year lifetime)
- tension...
  - ➡ **minimize material** for most precise measurements and to minimize interactions before the calorimeter
  - ➡ increasing **sensor granularity** to reduce occupancy
    - increase number of electronics channels and heat load
    - more material
- technology choices
  - ➡ **silicon detectors**, usually pixels for vertexing, and strips for tracking
    - good spatial resolution, high granularity, fast signal response
    - thin detector gives a large signal
  - ➡ can be complemented by **gas detectors** further away from vertex

Additional Roles of Tracker at LHC

- tracker also contribute to particle identification (PID)
  - ➡ use dedicated detectors to distinguish different particle types
    - Transition Radiation detectors also contribute to tracking
    - Ring Imaging Cherenkov detectors
    - time of flight
- match tracks with showers in the calorimeter
  - ➡ identify electrons from characteristic shower shape
- match central tracks with muon chamber segments
  - ➡ muon chamber information improves muon momentum measurement

Overall Design Choices

- **ATLAS and CMS** are general purpose detectors
  - ➡ central tracker covers $|\eta|<2.5$
    (polar angle expressed as pseudorapidity: $\eta = -\ln \tan(\Theta/2)$)
- **ALICE** - optimized for heavy ions, high occupancy
  - ➡ tracker restricted to $|\eta|<0.9$, plus forward muons
- all three are symmetric about the interaction point
  - ➡ solenoid magnet providing uniform magnetic field parallel to the beam direction
  - ➡ ATLAS Muon Spectrometer is in field of 3 toroid magnets
- **LHCb** - beauty-hadron production in forward direction
  - ➡ despite the different geometry, design is driven by the same principles to give optimal performance
  - ➡ tracker is not in a magnetic field, tracks are measured before and after a dipole magnet

Overall Design Choices

- layout of the tracking detectors
  - ➡ follow the typical geometry of fix target and collider experiments

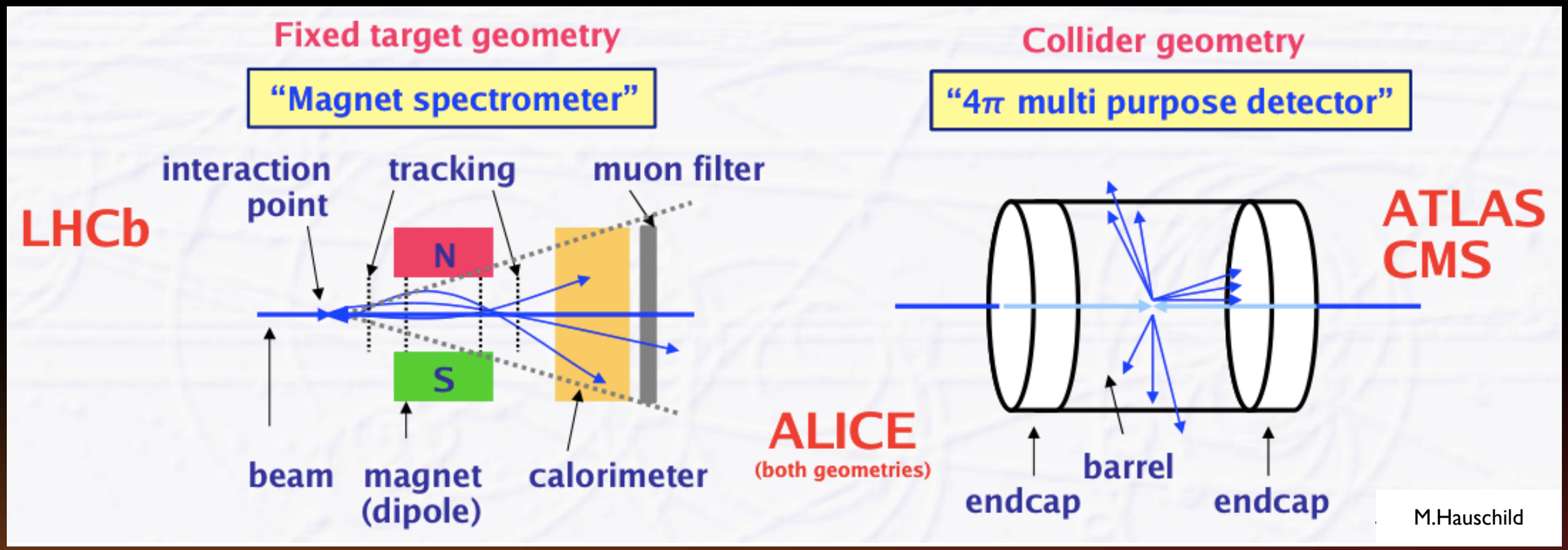

Semiconductor Trackers

Semiconductors

Semiconductors

- doping of silicon crystal semiconductors:

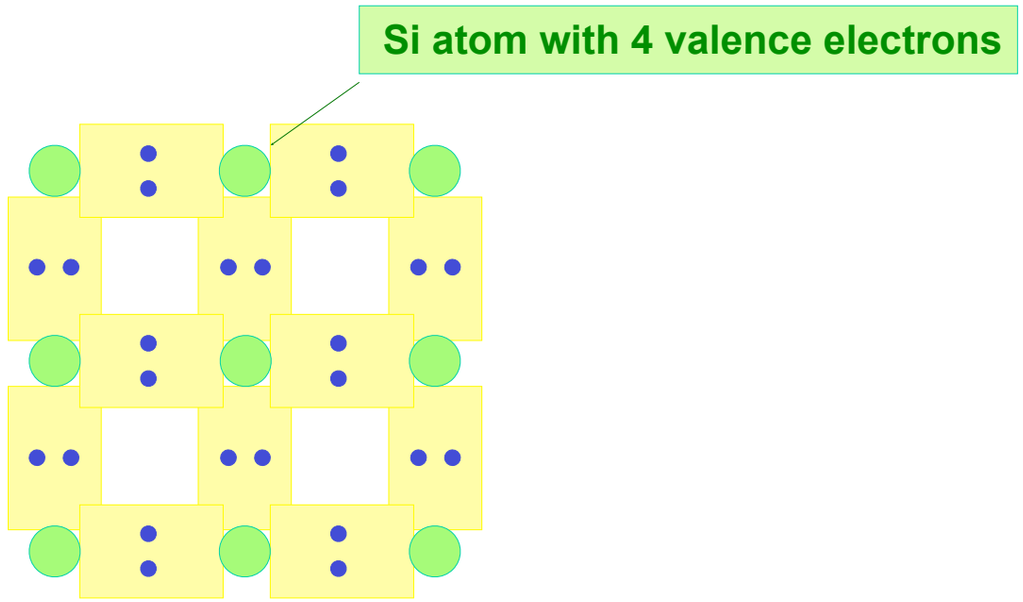

Semiconductors

- doping of silicon crystal semiconductors:

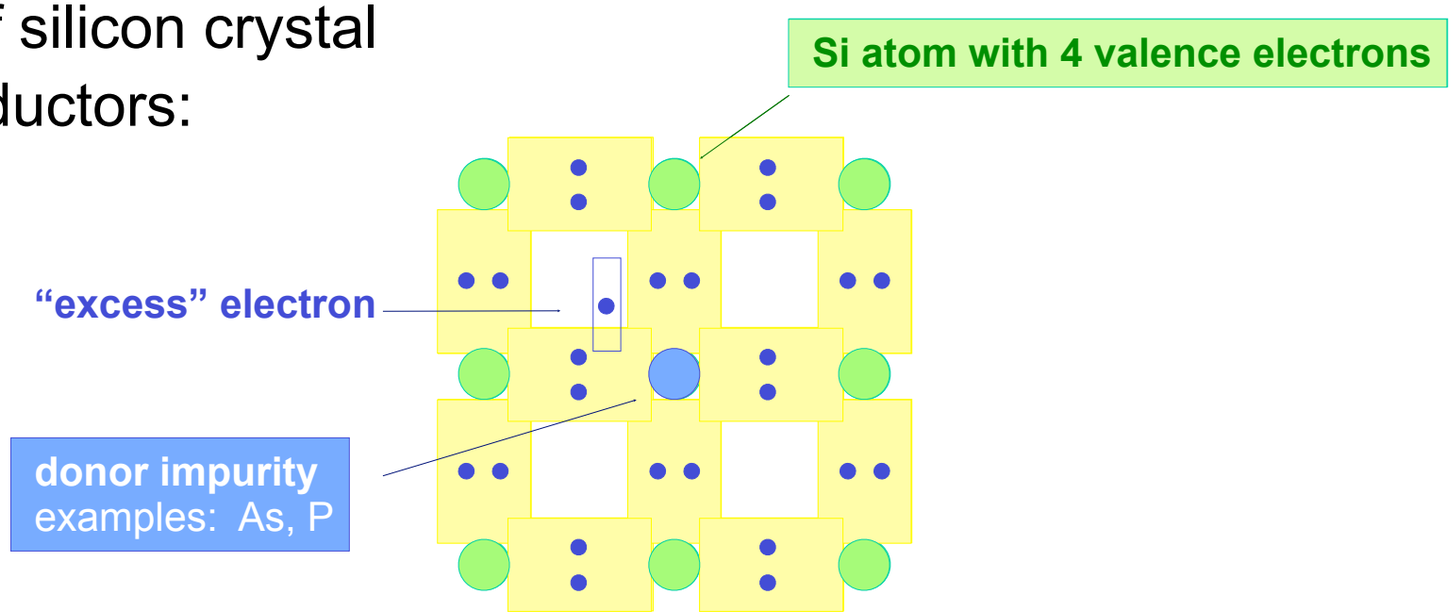

Semiconductors

- doping of silicon crystal semiconductors:

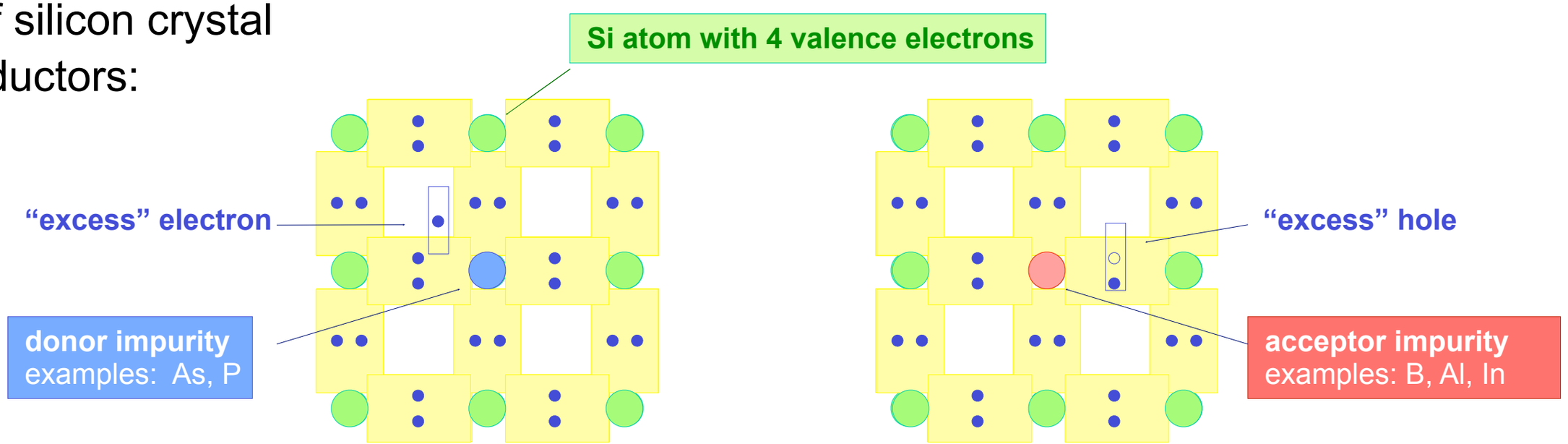

Semiconductors

- doping of silicon crystal semiconductors:

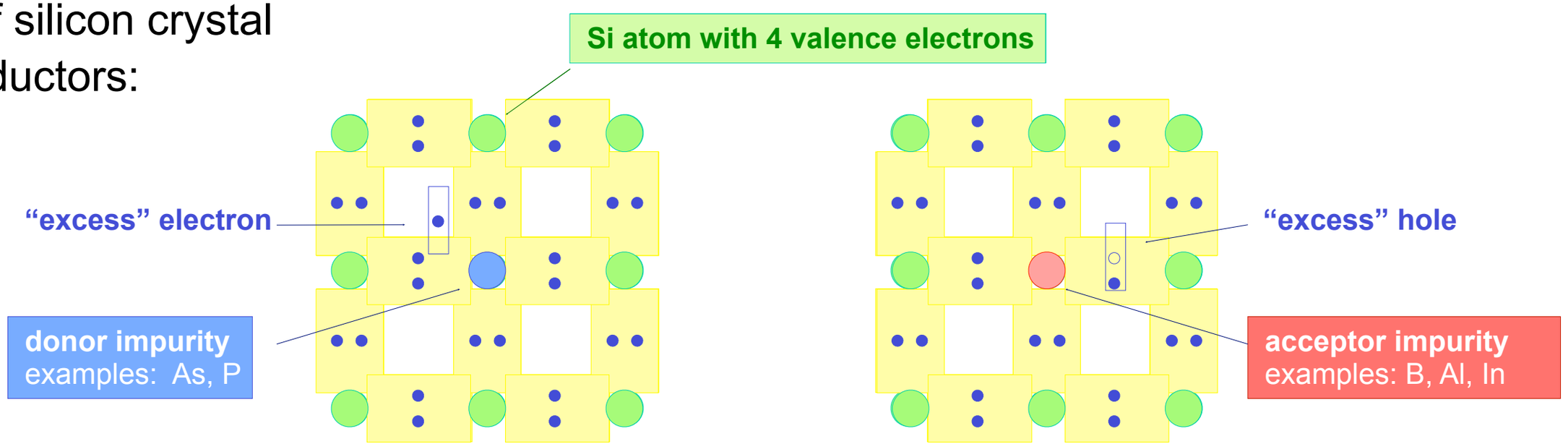

p–n junction

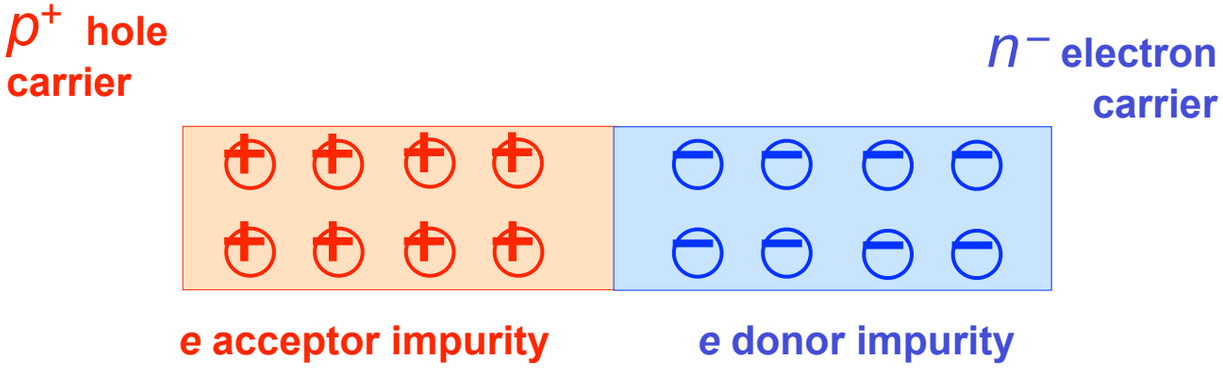

- *p* doping adds electro-phile atoms
- *n* doping adds electro-phobe atoms

Semiconductors

- doping of silicon crystal semiconductors:

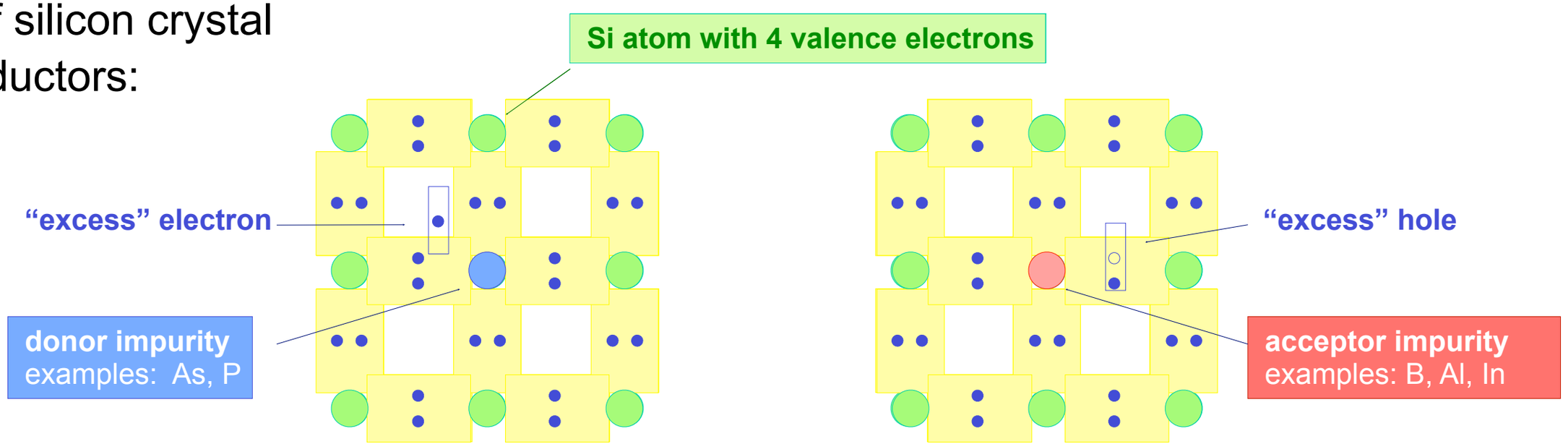

p–n junction

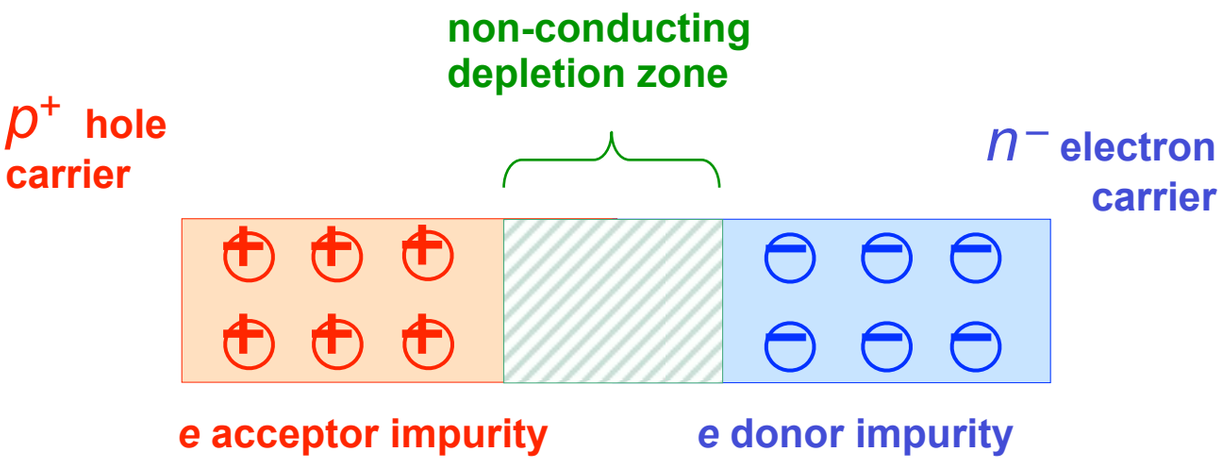

- in the junction zone, electron-hole pairs recombine creating depletion
- the potential barrier in the junction counter-weighs the doping potential

Semiconductors

- doping of silicon crystal semiconductors:

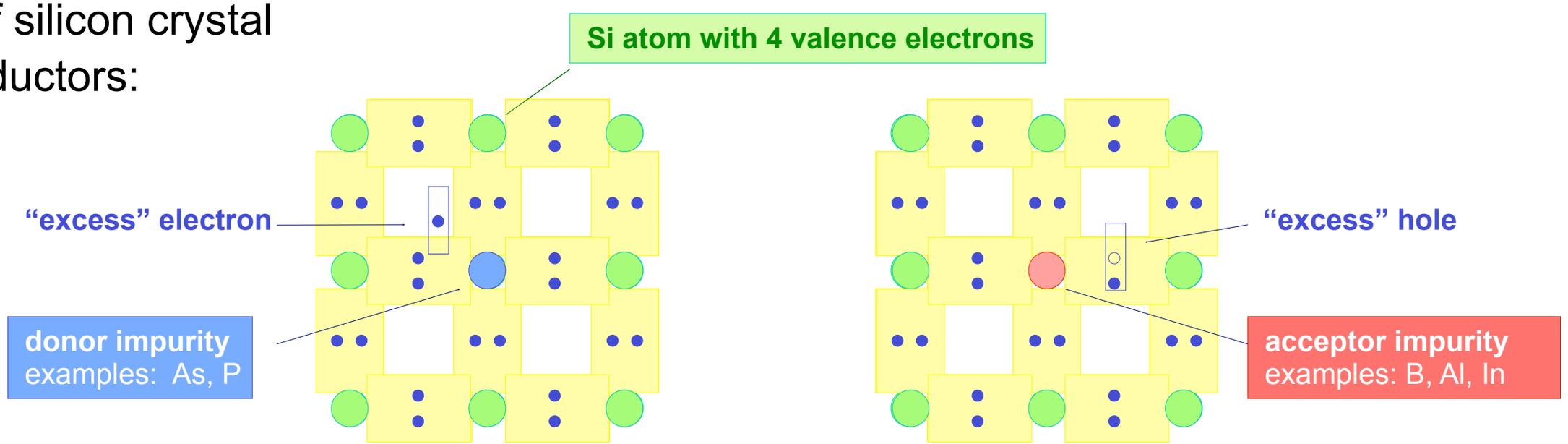

reverse bias *p*–*n* junction

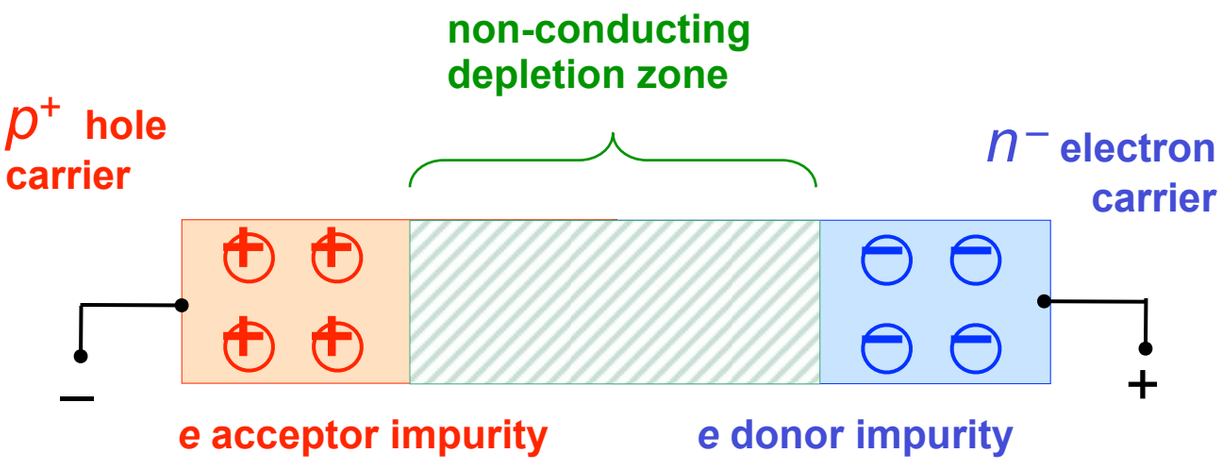

- the reversed bias voltage increases the potential barrier in the depletion zone, enhancing its resistance
- minimal current across the junction

The *p*–*n* Junction as a Tracking Detector

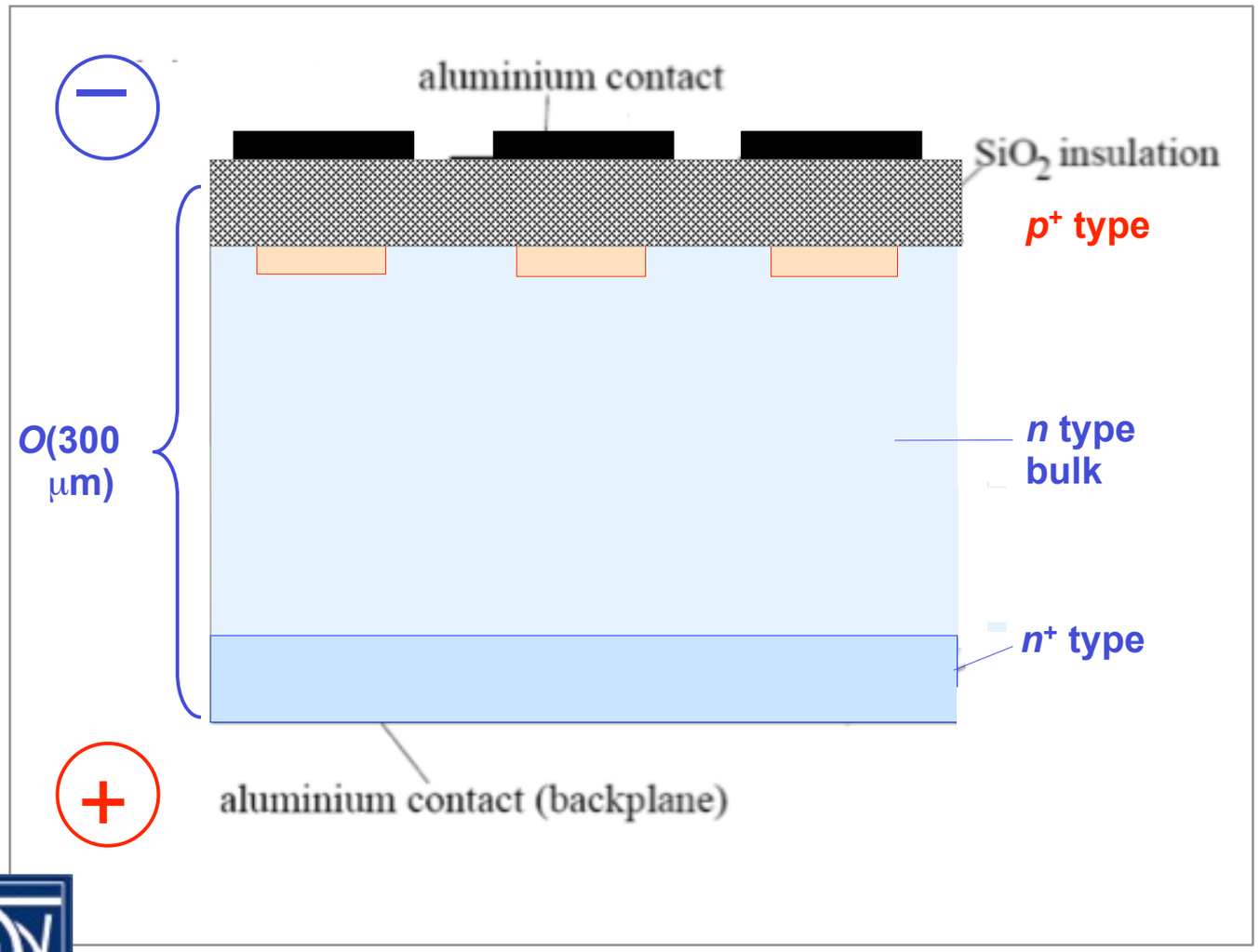

The *p*–*n* Junction as a Tracking Detector

- thin (~μm), highly doped p^+ (~10^{19} cm^{-3}) layer on lightly doped n (~10^{12} cm^{-3}) substrate
- high mobility of charge carriers in Si allows fast charge collection (~5 ns for electron)
- high Si density & low electron–hole creation potential (3.6 eV compared to ~36 eV for gaseous ionization) allows use of very thin detectors with reasonable signal

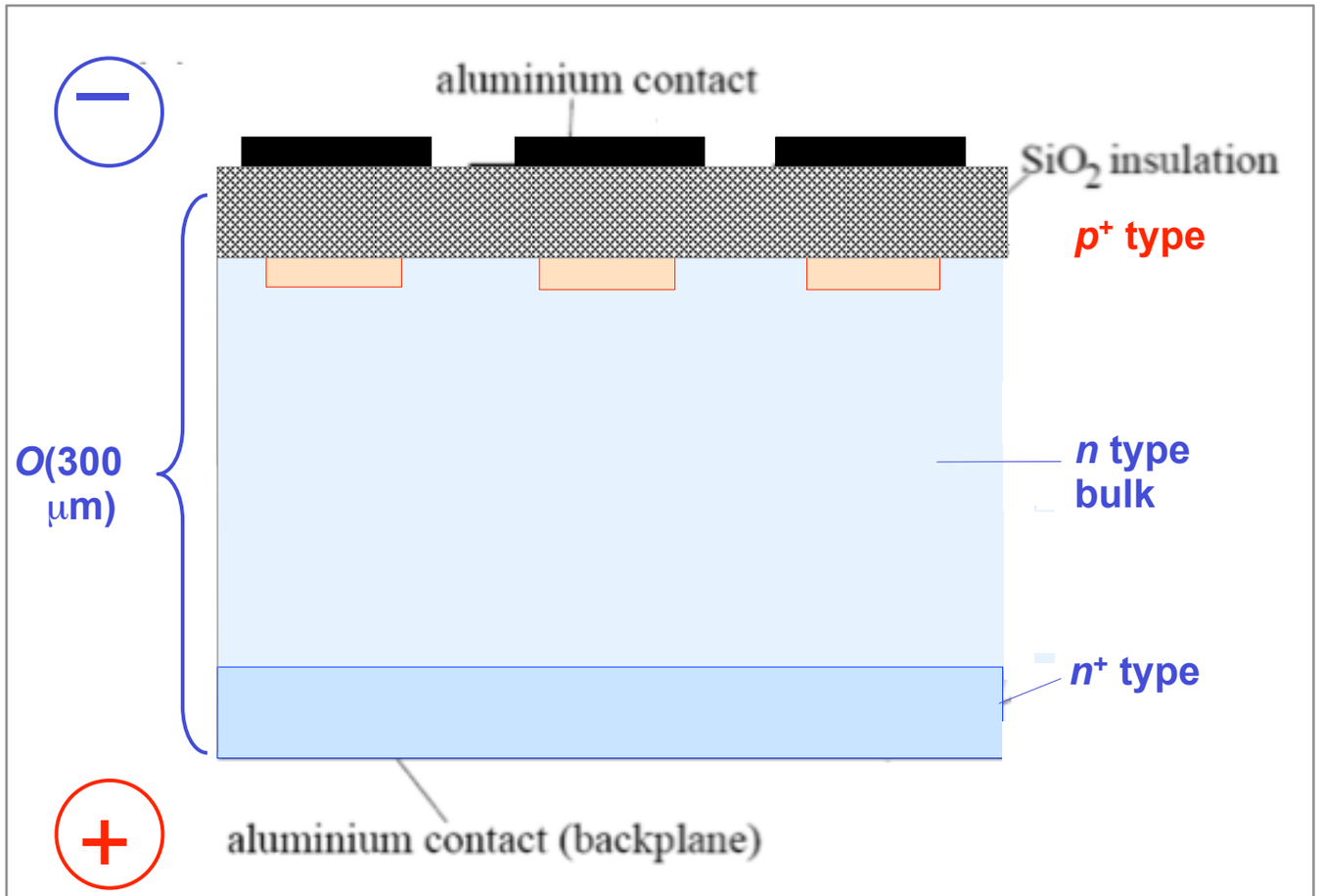

schema of silicon microstrip sensor

- reverse bias: backplane set to positive voltage (< 500 V)
- a traversing charged particle ionizes silicon, creating conduction electrons and holes that induce a measurable current by drifting to electrodes
- metal-semiconductor transition forms charge (Schottky) barrier similar to *p*–*n* junction. Highly doped n^+ layer reduces width of potential barrier and hence resistance

The *p*–*n* Junction as a Tracking Detector

- thin (~μm), highly doped p^+ (~10^{19} cm^{-3}) layer on lightly doped n (~10^{12} cm^{-3}) substrate
- high mobility of charge carriers in Si allows fast charge collection (~5 ns for electron)
- high Si density & low electron–hole creation potential (3.6 eV compared to ~36 eV for gaseous ionization) allows use of very thin detectors with reasonable signal

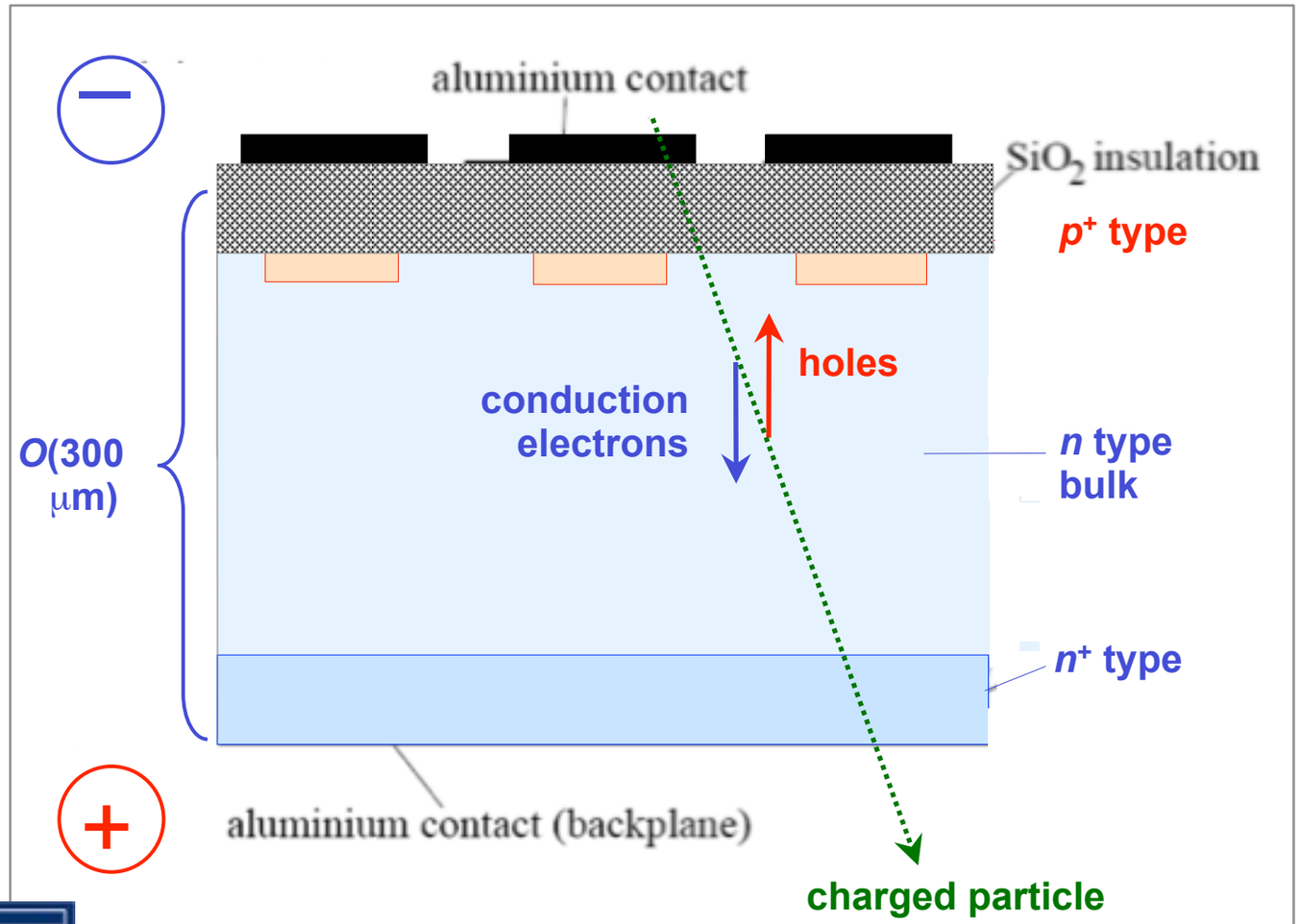

schema of silicon microstrip sensor

- reverse bias: backplane set to positive voltage (< 500 V)
- a traversing charged particle ionizes silicon, creating conduction electrons and holes that induce a measurable current by drifting to electrodes
- metal-semiconductor transition forms charge (Schottky) barrier similar to *p*–*n* junction. Highly doped n^+ layer reduces width of potential barrier and hence resistance

Lorentz Angle Measurement

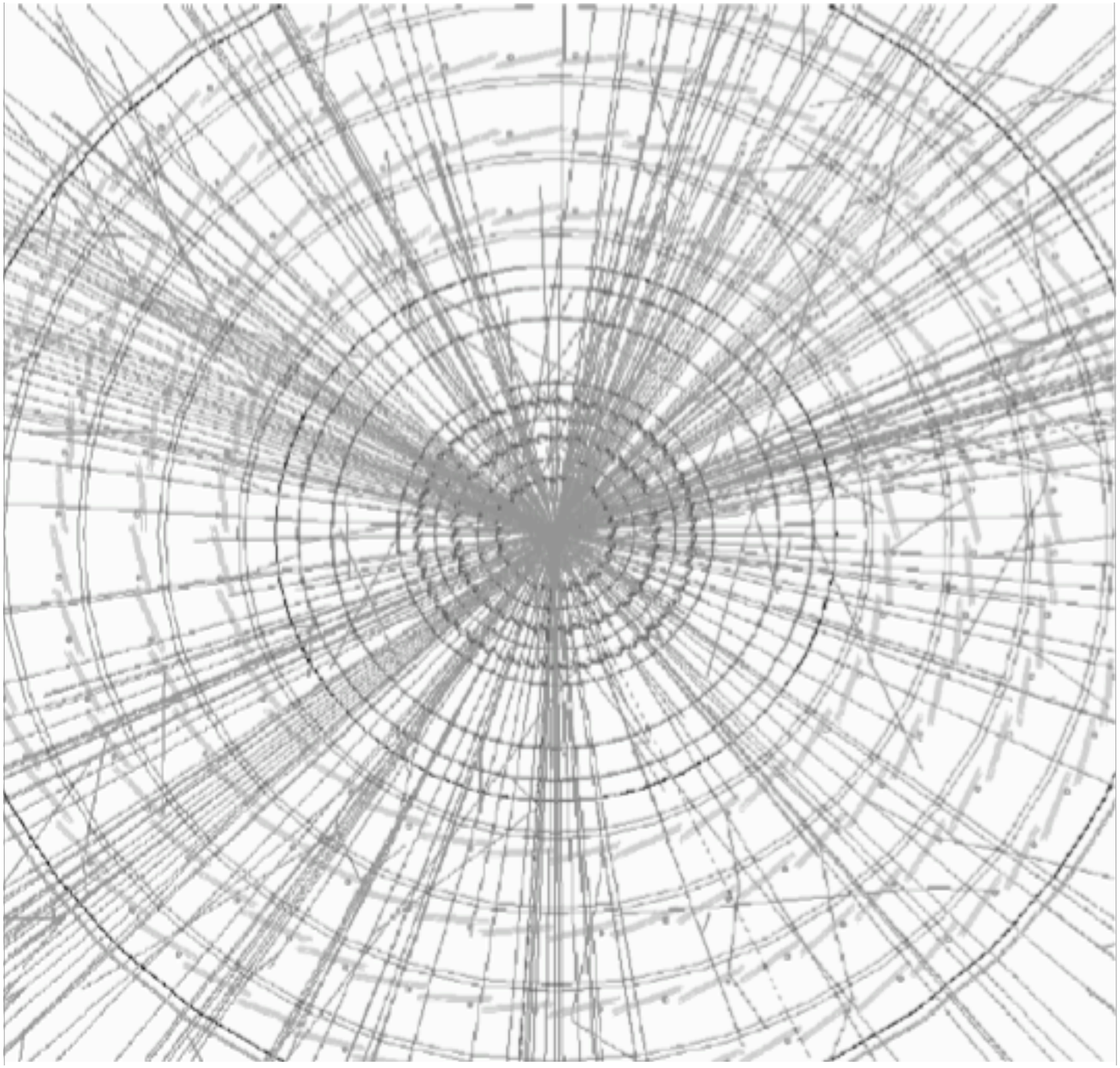

Lorentz Angle Measurement

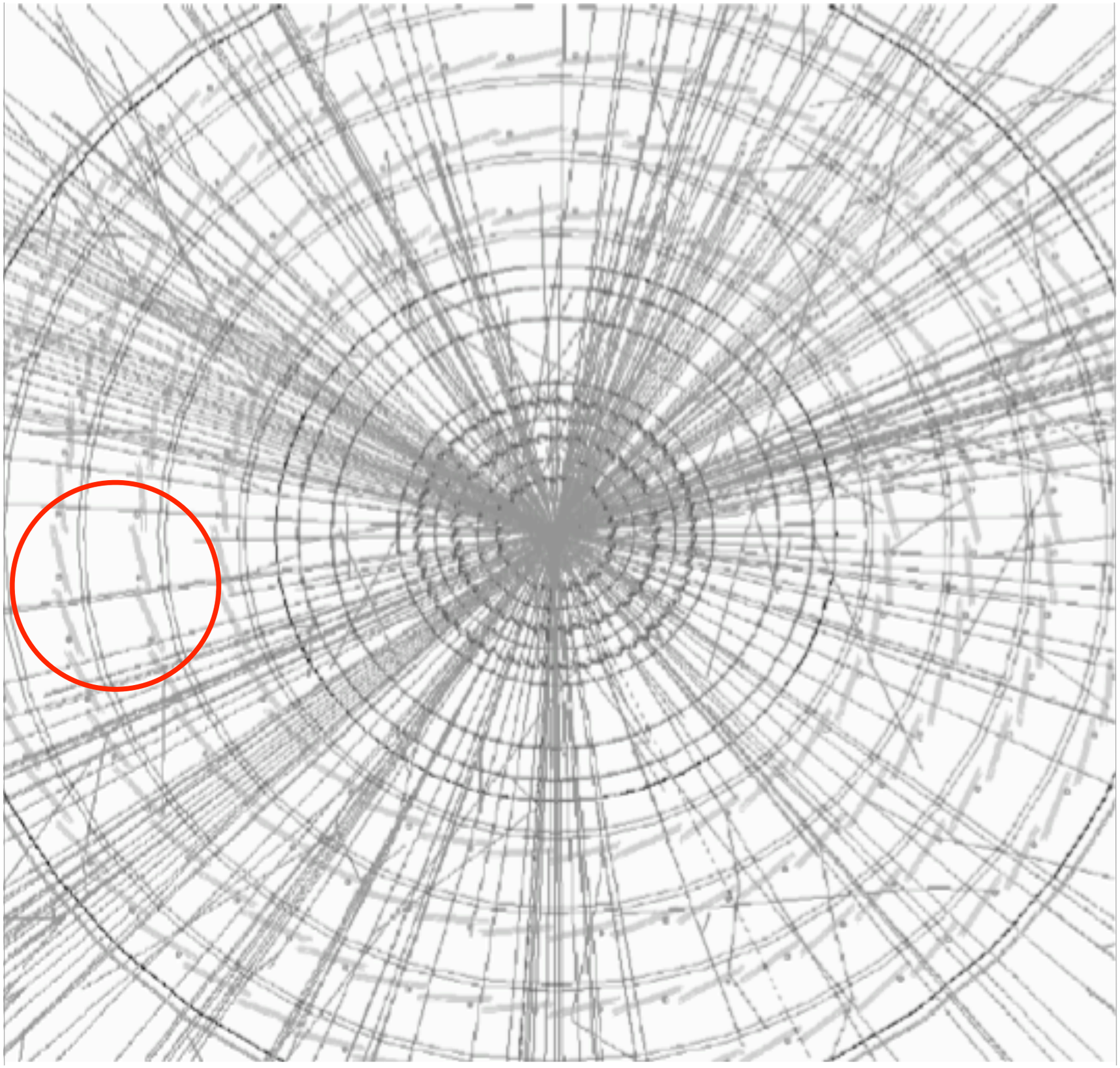

Lorentz Angle Measurement

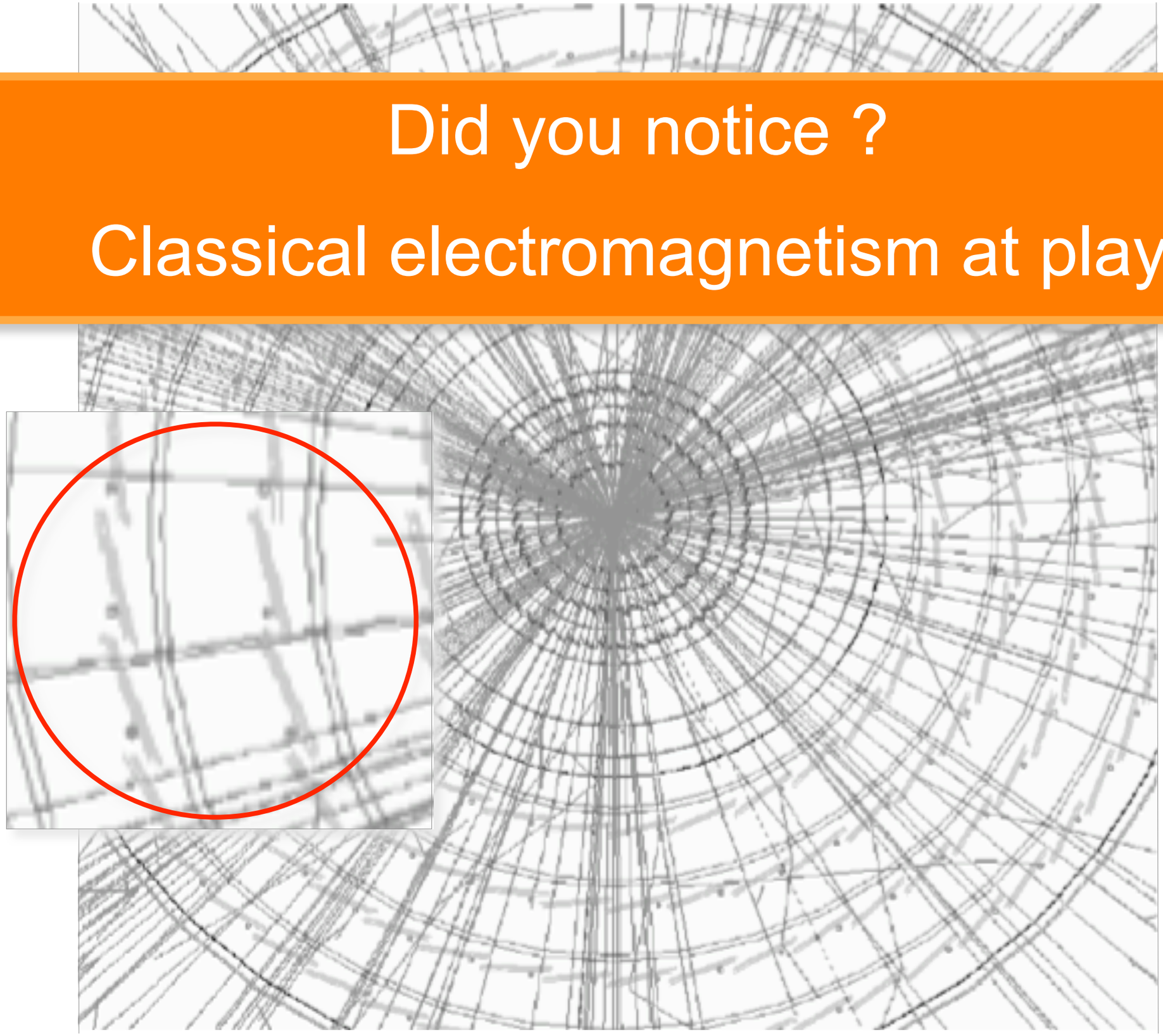

Did you notice ?

Classical electromagnetism at play!

Lorentz Angle Measurement

- the sensors are tilted relative to the pointing axis: SCT (11°) and Pixel (-20°) (*)
  - the charges traveling through the Si substrate are deviated by 2T *B* field (Hall effect)

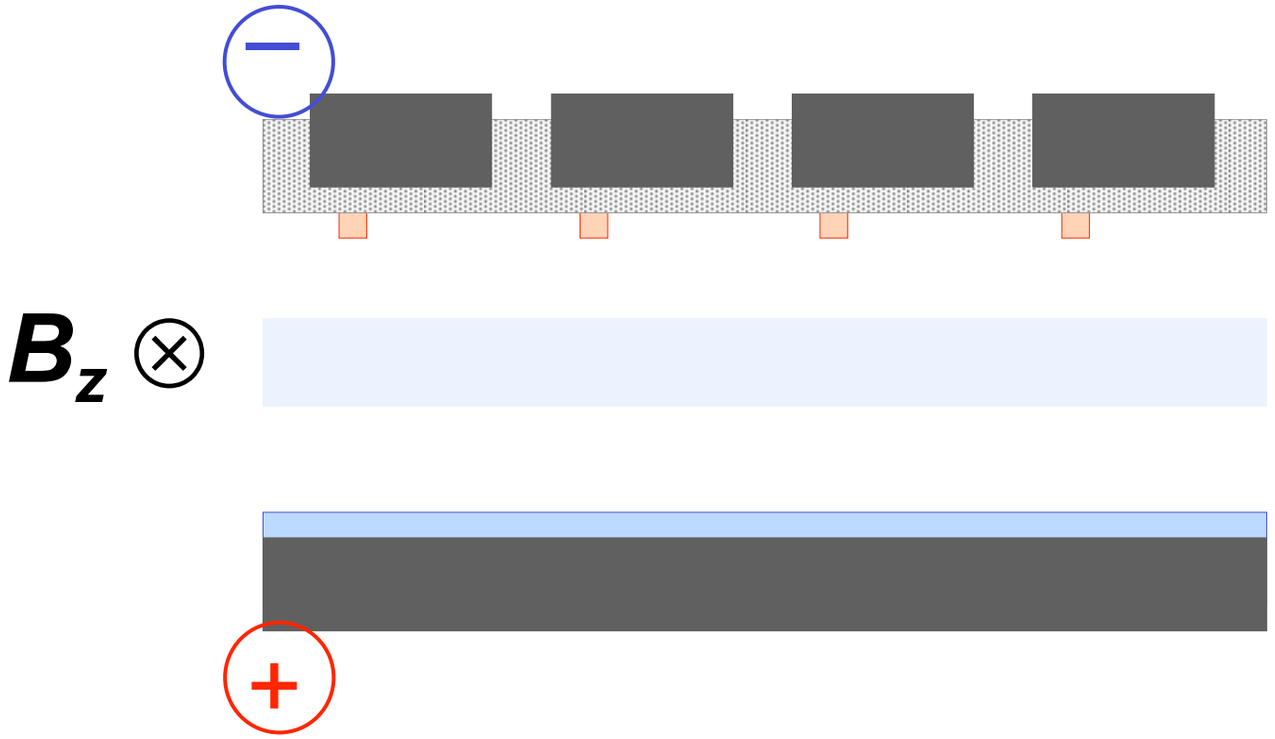

(*) The actual Pixel and SCT Lorentz angles are 4° and 12° (no irradiation), and with opposite signs. The tilts chosen are due to technical reasons.

Lorentz Angle Measurement

- the sensors are tilted relative to the pointing axis: SCT (11°) and Pixel (-20°) (*)
  - the charges traveling through the Si substrate are deviated by 2T *B* field (Hall effect)

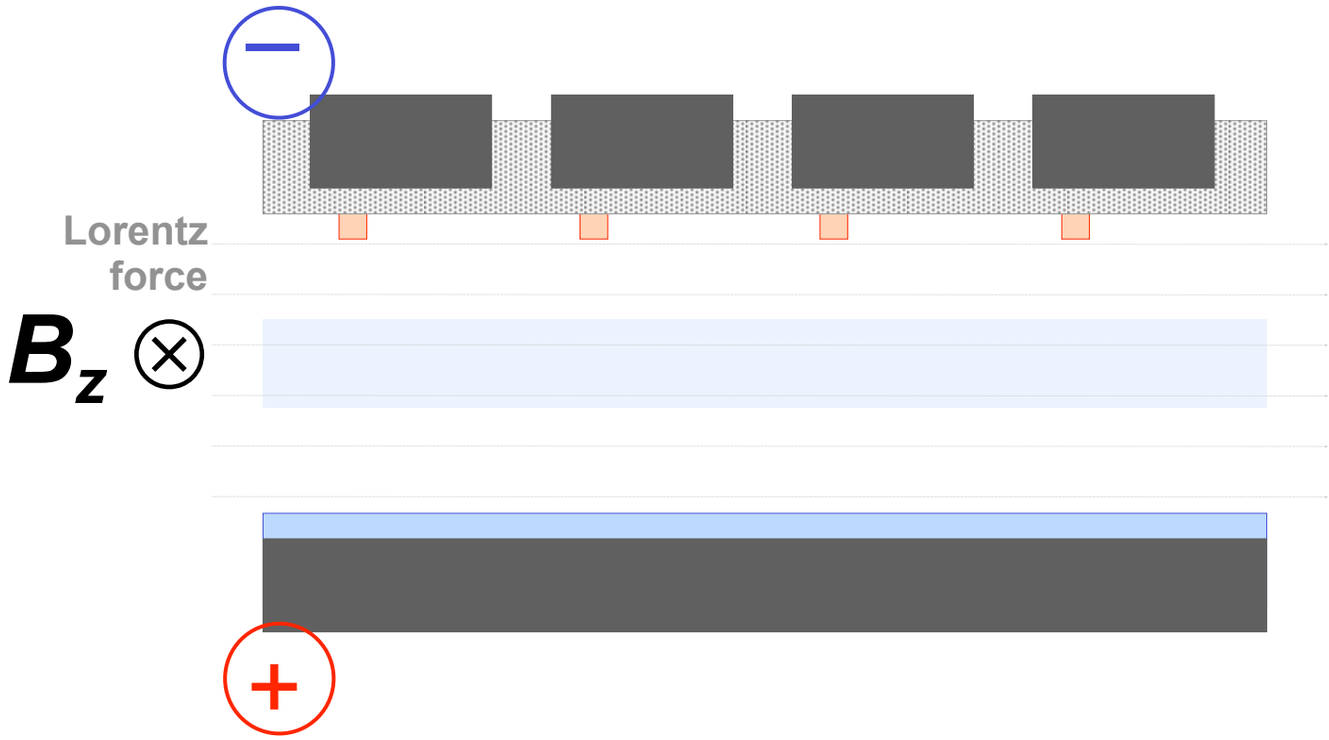

(*) The actual Pixel and SCT Lorentz angles are 4° and 12° (no irradiation), and with opposite signs. The tilts chosen are due to technical reasons.

Lorentz Angle Measurement

- the sensors are tilted relative to the pointing axis: SCT (11°) and Pixel (-20°) (*)
  - the charges traveling through the Si substrate are deviated by 2T *B* field (Hall effect)

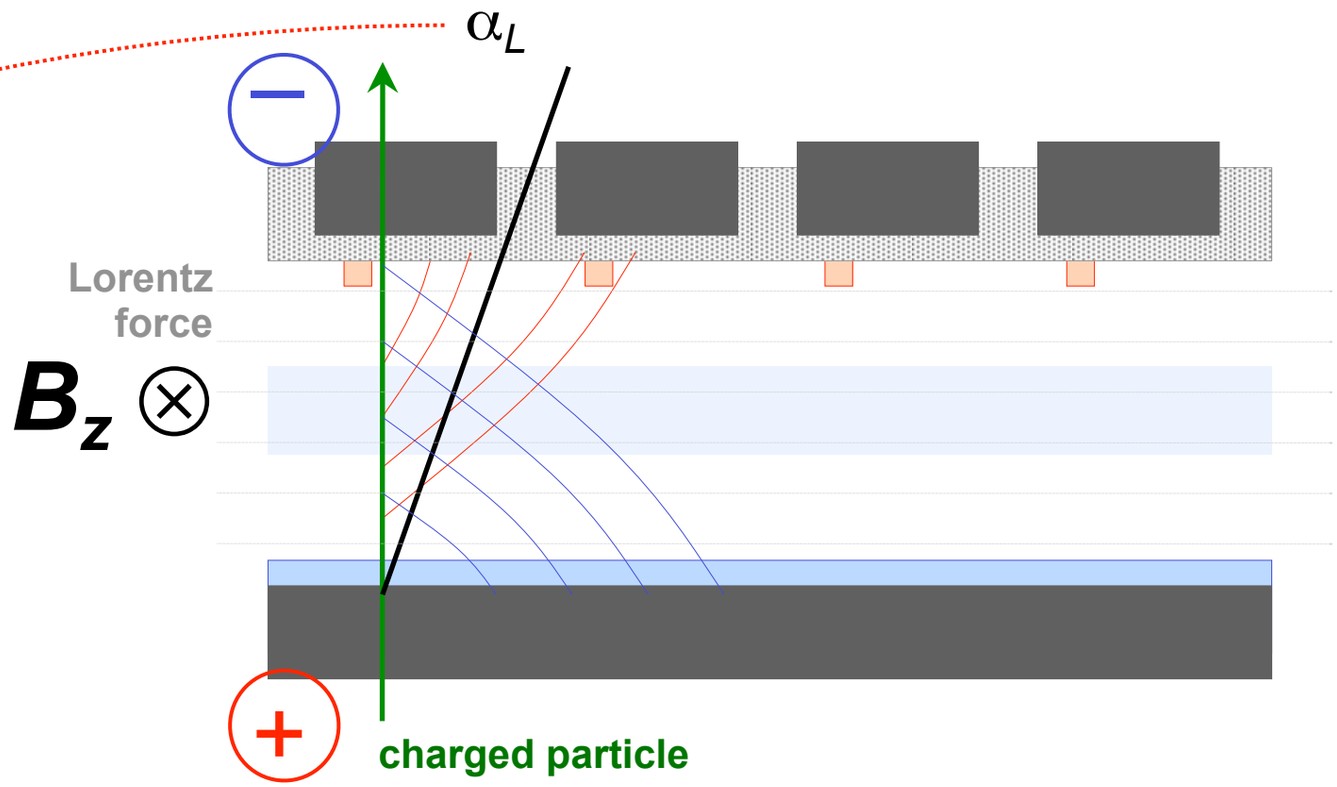

(*) The actual Pixel and SCT Lorentz angles are 4° and 12° (no irradiation), and with opposite signs. The tilts chosen are due to technical reasons.

Lorentz Angle Measurement

- the sensors are tilted relative to the pointing axis: SCT (11°) and Pixel (-20°) (*)
  - the charges traveling through the Si substrate are deviated by 2T *B* field (Hall effect)

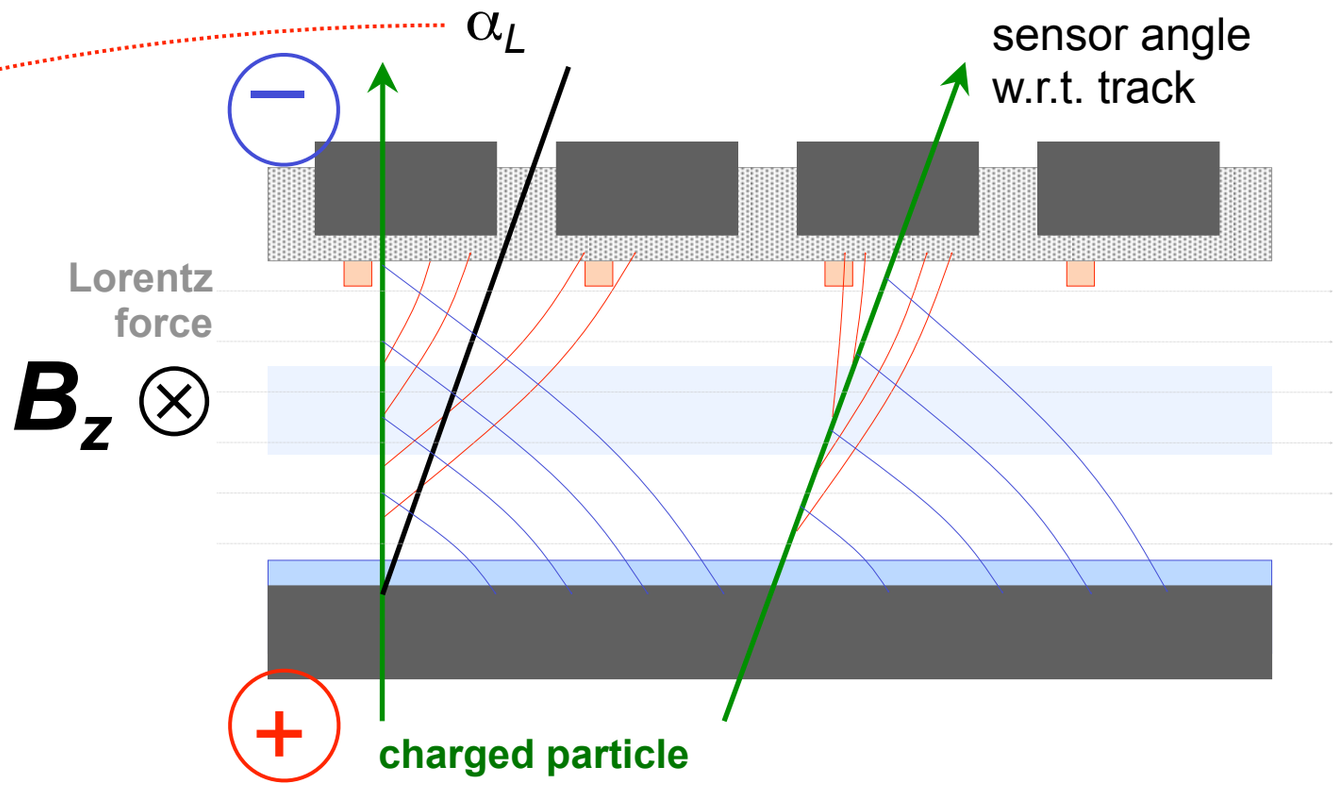

- Lorentz angle determined empirically in test beam by minimizing cluster size
- $\alpha_L = f(V_{depl})$ → as bias voltage increases to cope with irradiation, α_L decreases

(*) The actual Pixel and SCT Lorentz angles are 4° and 12° (no irradiation), and with opposite signs. The tilts chosen are due to technical reasons.

Pixel Sensors in Radiation Environment

- non-ionizing energy loss (NIEL) from irradiation causes irreversible Si lattice damage
  - increase of leakage current (linear), effective *p* doping, trapping of signal charge
  - “type inversion” of the bulk

Pixel Sensors in Radiation Environment

- non-ionizing energy loss (NIEL) from irradiation causes irreversible Si lattice damage
  - increase of leakage current (linear), effective *p* doping, trapping of signal charge
  - “type inversion” of the bulk

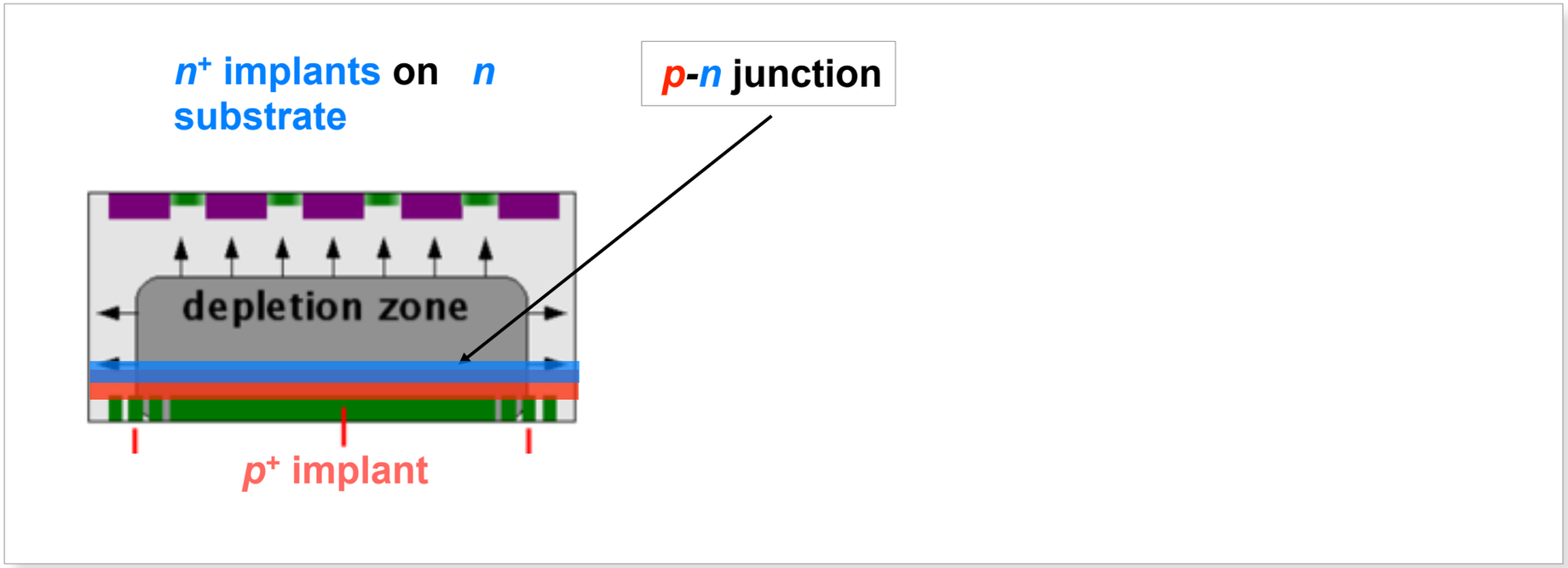

Pixel Sensors in Radiation Environment

- non-ionizing energy loss (NIEL) from irradiation causes irreversible Si lattice damage
  - increase of leakage current (linear), effective *p* doping, trapping of signal charge
  - “type inversion” of the bulk

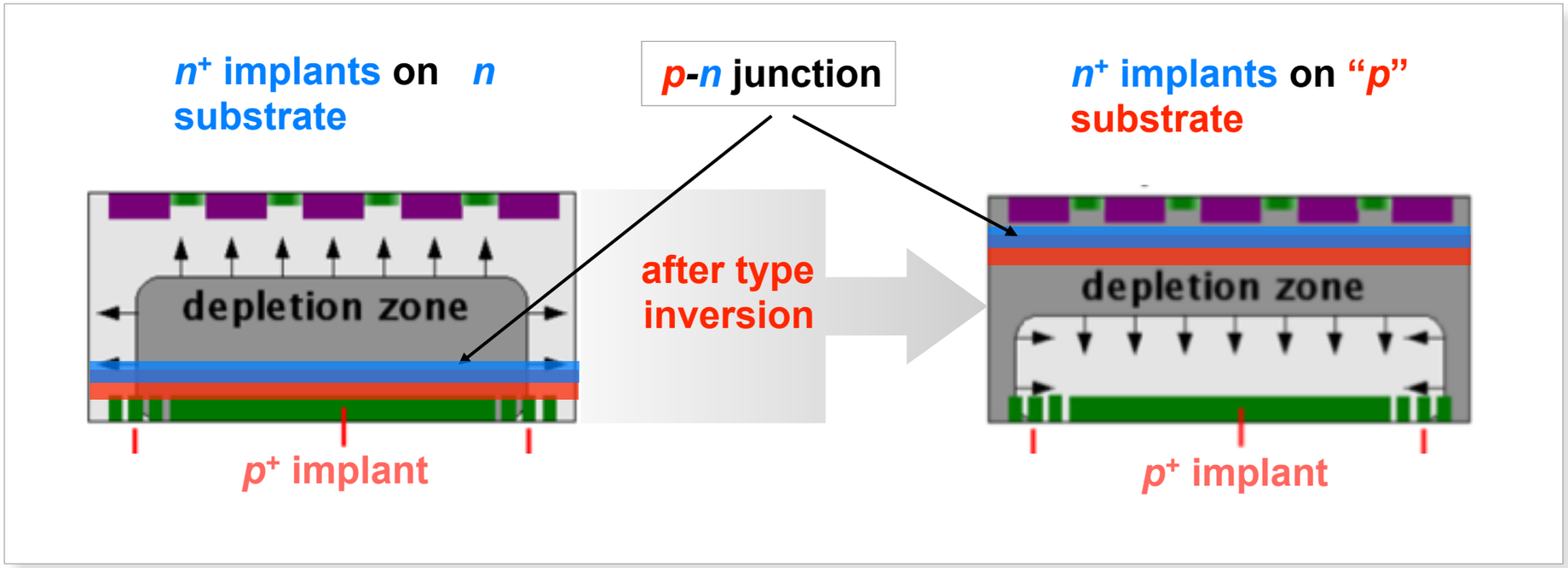

Pixel Sensors in Radiation Environment

- non-ionizing energy loss (NIEL) from irradiation causes irreversible Si lattice damage
  - increase of leakage current (linear), effective *p* doping, trapping of signal charge
  - “type inversion” of the bulk

change of depletion voltage with particle fluence

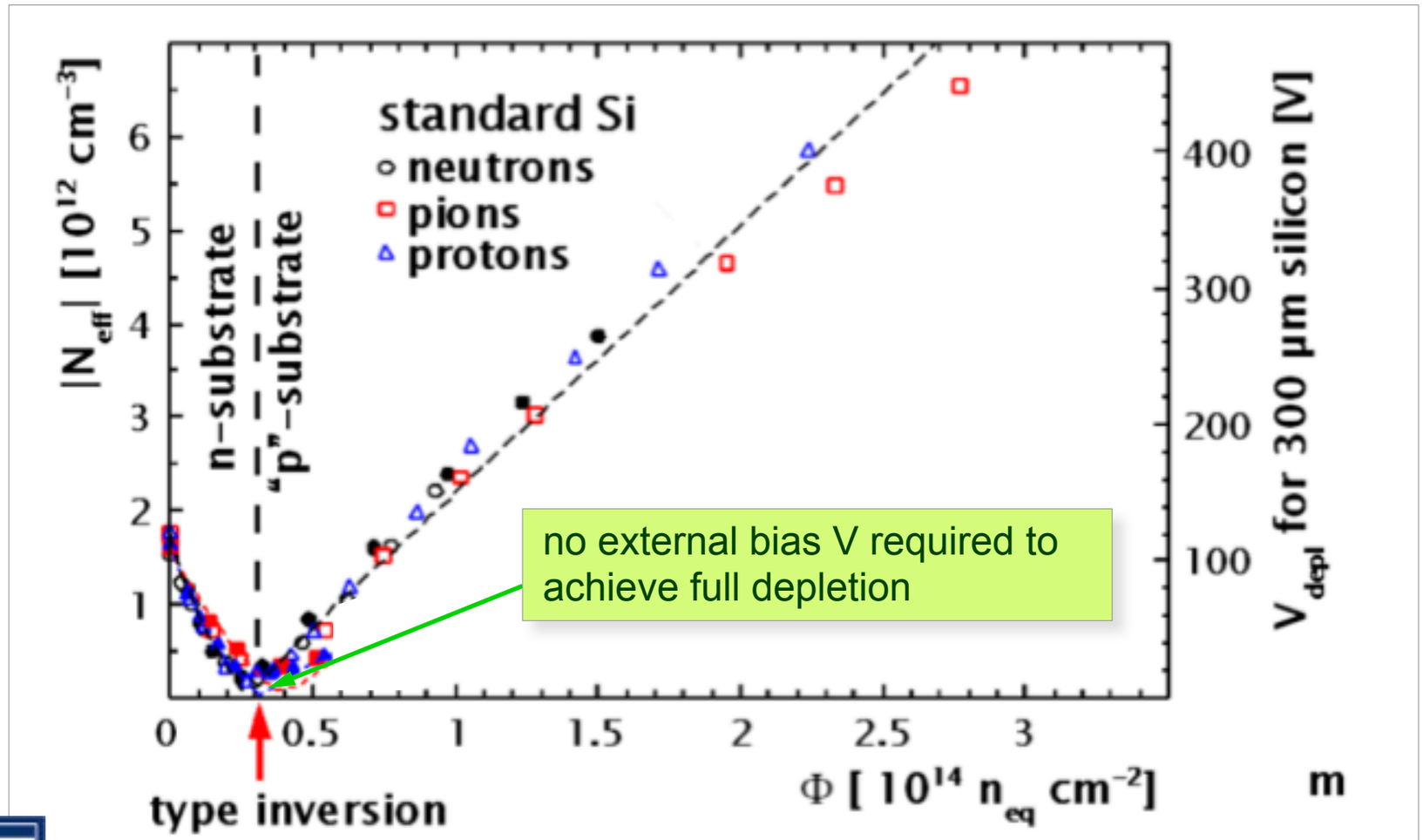

Pixel Sensors in Radiation Environment

- non-ionizing energy loss (NIEL) from irradiation causes irreversible Si lattice damage
  - increase of leakage current (linear), effective *p* doping, trapping of signal charge
  - “type inversion” of the bulk

change of depletion voltage with particle fluence

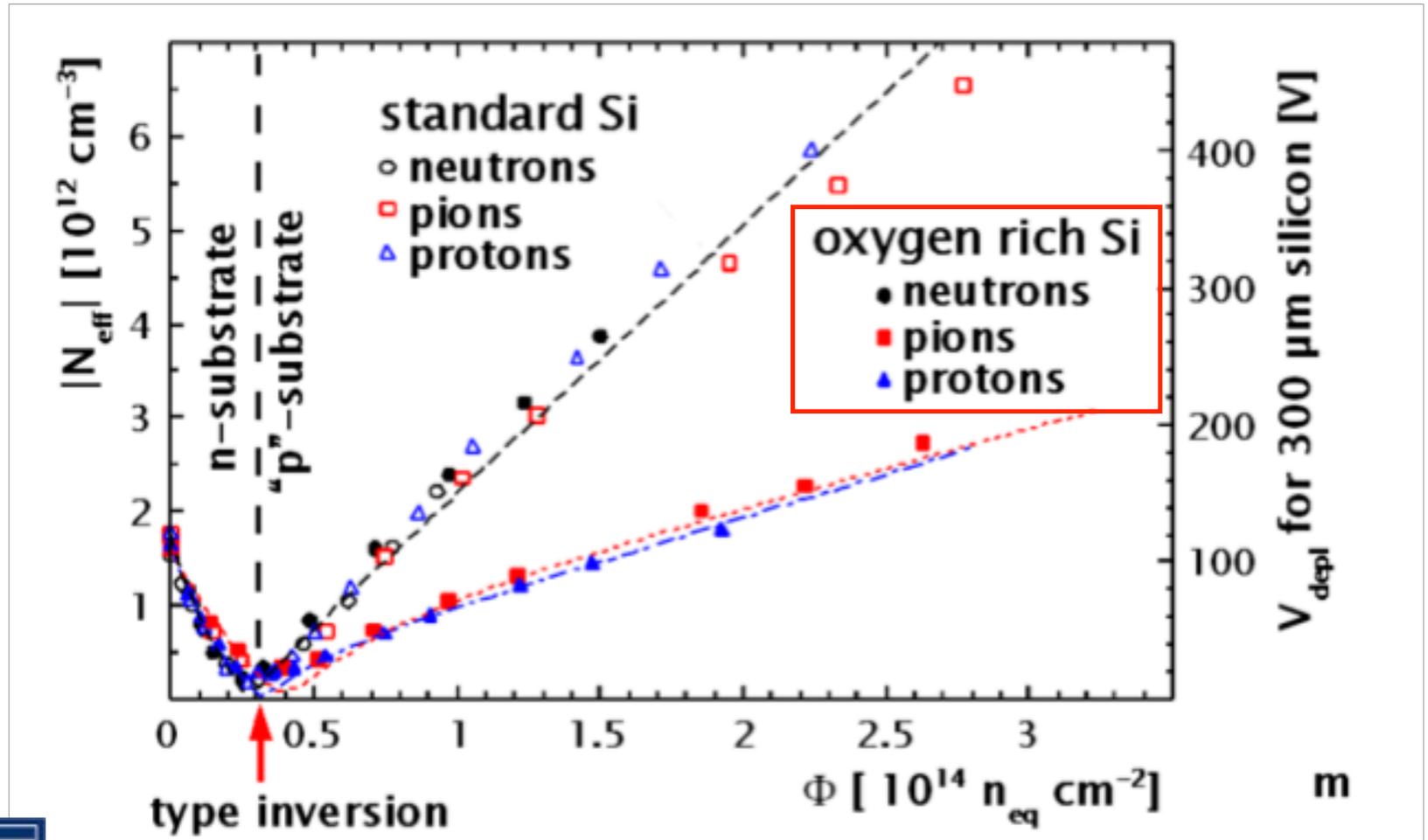

Si oxygenation: keeps required bias voltage for full depletion within operational 600 V for ~10 yrs

CMS Tracker

- largest silicon tracker ever built
  - ➡ **Pixels:** 66M channels, 100x150 μm^2 Pixel
  - ➡ **Si-Strip detector:** ~23m^3, 210m^2 of Si area, 10.7M channels

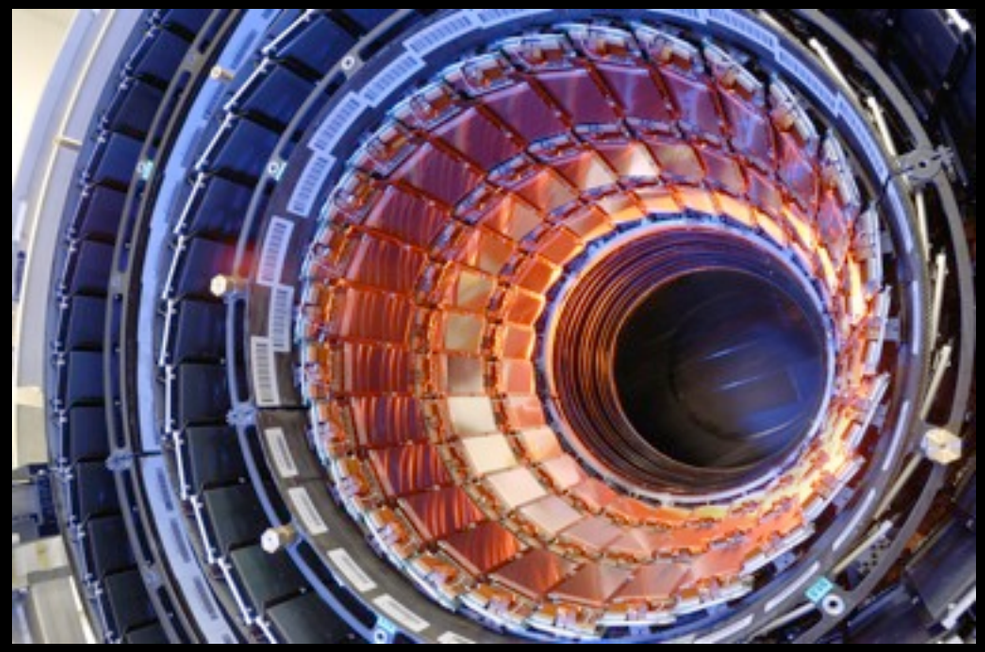

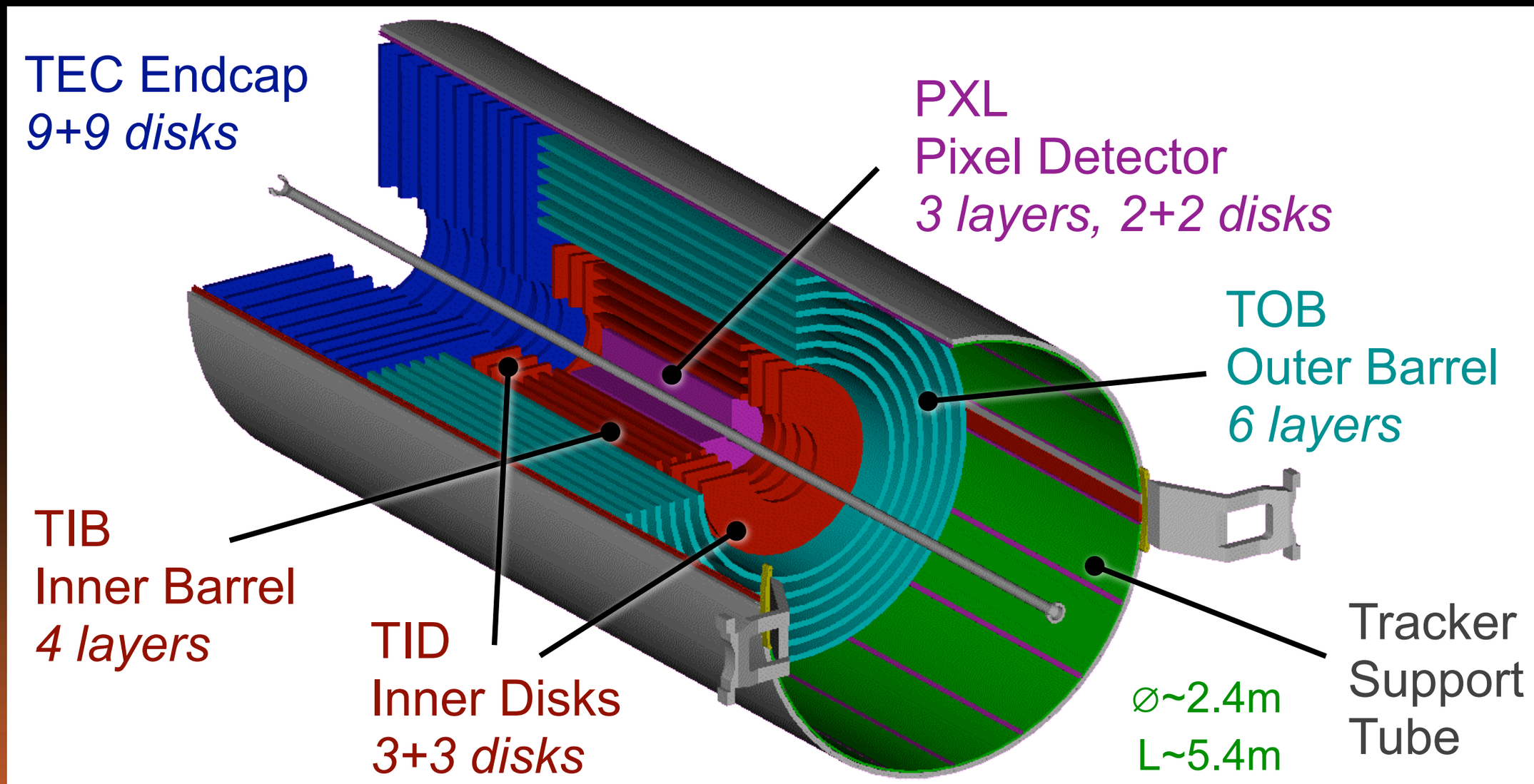

Drift Tubes in ATLAS: Inner Detector and Muon Spectrometer

- classical detection technique for charged particles based on gas ionization and drift time measurement

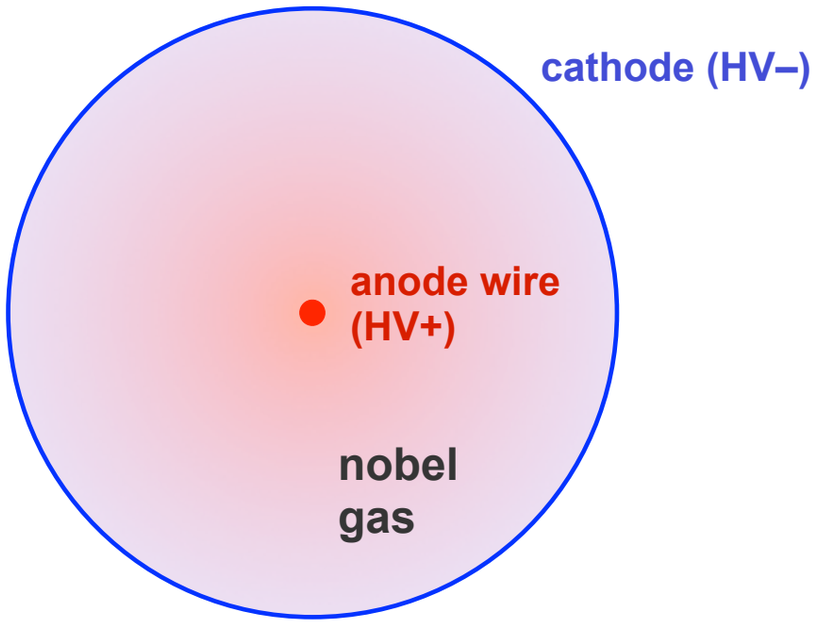

Drift Tubes in ATLAS: Inner Detector and Muon Spectrometer

- classical detection technique for charged particles based on gas ionization and drift time measurement

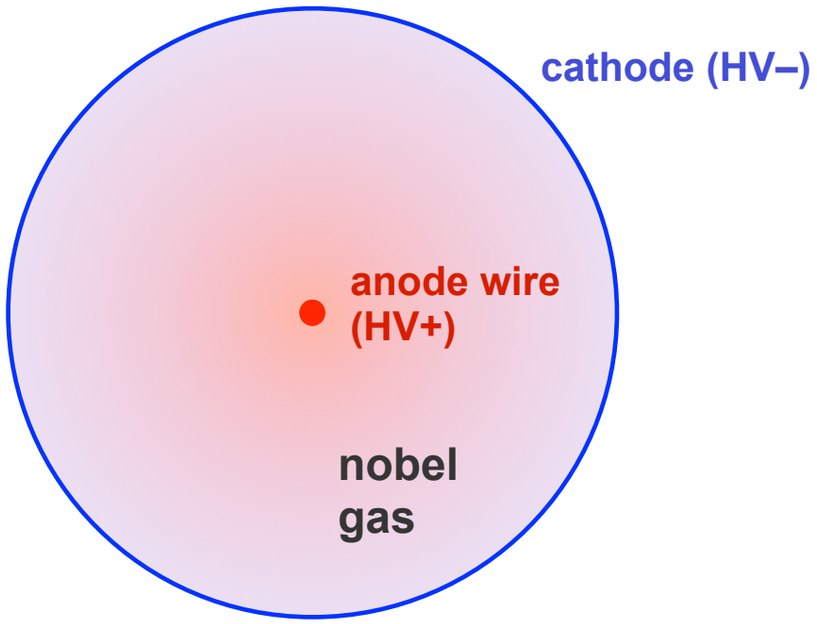

- drift tubes used in muon systems and ATLAS TRT
- primary electrons drift towards thin anode wire
- charge amplification during drift (~10^4) in high E-field in vicinity of wire: $E(r) \sim U_0 / r$
- signal rises with number of primary e's (dE/dx) [signal dominated by ions]
- macroscopic drift time: $v_D / c \sim 10^{-4} \rightarrow \sim 30$ ns/mm
- determine v_D from difference between signal peaking time and expected particle passage
- spatial resolution of $O(100\ \mu m)$

TRT: Kapton tubes, ∅ = 4 mm
MDT: Aluminium tubes, ∅ = 30 mm

Drift Tubes in ATLAS: Inner Detector and Muon Spectrometer

- classical detection technique for charged particles based on gas ionization and drift time measurement

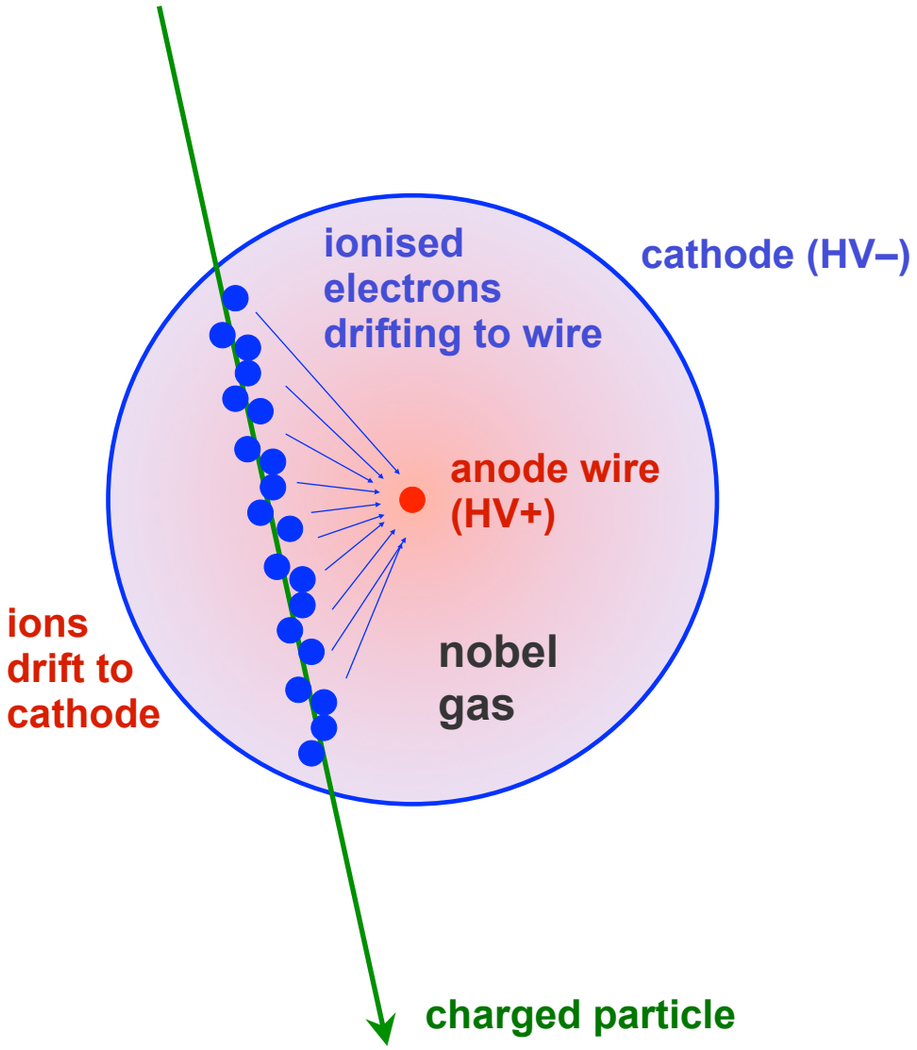

- drift tubes used in muon systems and ATLAS TRT
- primary electrons drift towards thin anode wire
- charge amplification during drift (~10^4) in high E-field in vicinity of wire: $E(r) \sim U_0 / r$
- signal rises with number of primary e's (dE/dx) [signal dominated by ions]
- macroscopic drift time: $v_D / c \sim 10^{-4} \rightarrow \sim 30$ ns/mm
- determine v_D from difference between signal peaking time and expected particle passage
- spatial resolution of $O(100\ \mu m)$

TRT: Kapton tubes, ∅ = 4 mm
MDT: Aluminium tubes, ∅ = 30 mm

Drift Tubes in ATLAS: Inner Detector and Muon Spectrometer

- classical detection technique for charged particles based on gas ionization and drift time measurement

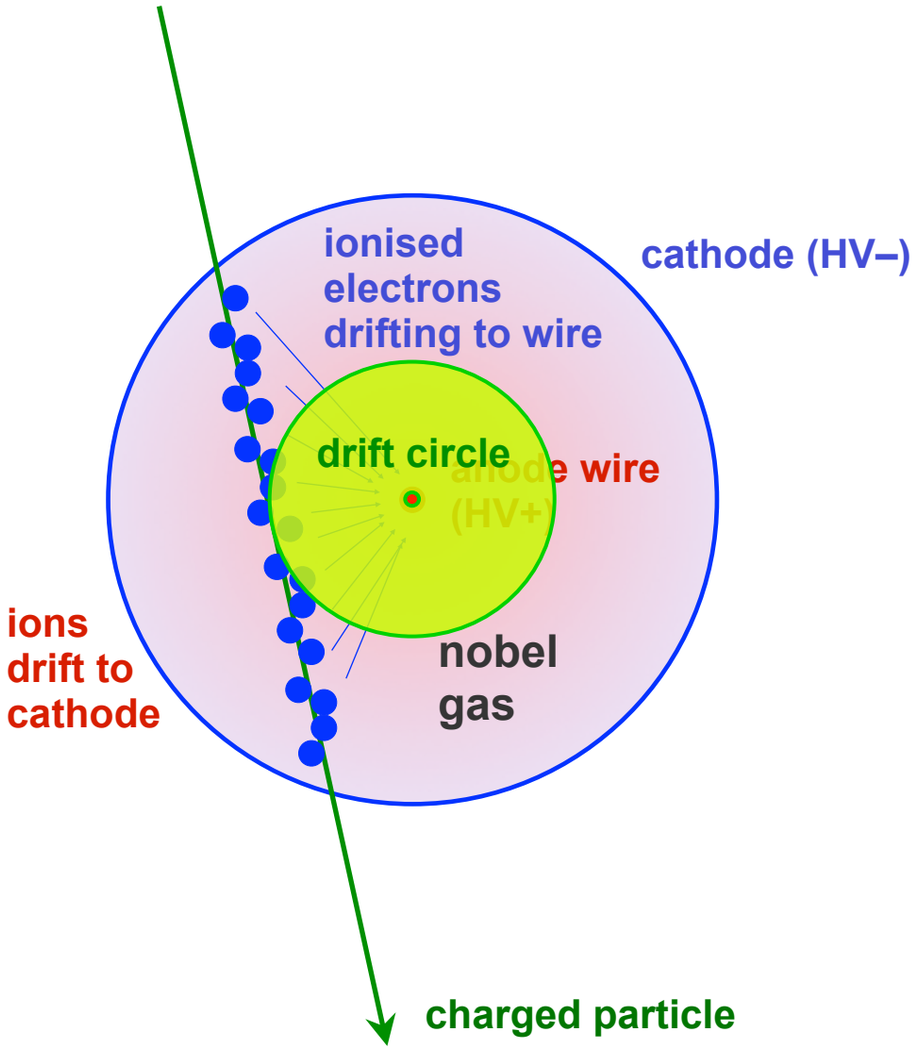

example: segment in muon drift tubes reconstruction from measured drift circles (left-right ambiguity)

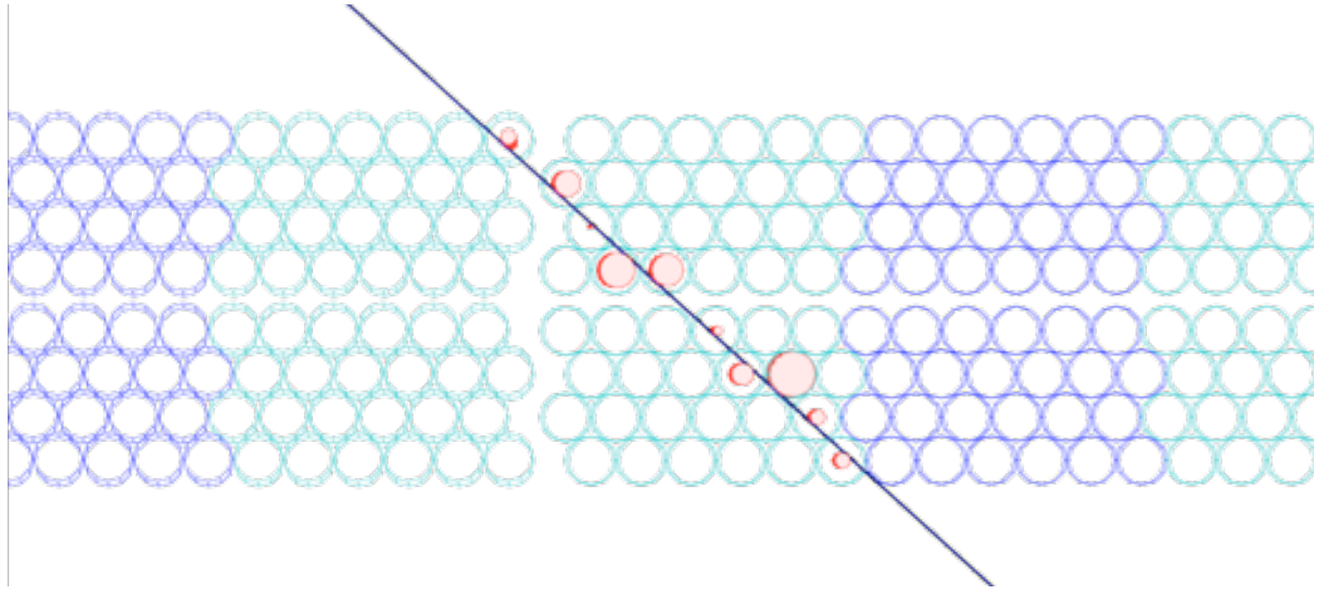

TRT: Kapton tubes, ∅ = 4 mm
MDT: Aluminium tubes, ∅ = 30 mm

Combining Tracking with PID: the ATLAS TRT

- e/π separation via transition radiation: polymer (PP) fibers/foils interleaved with drift tubes

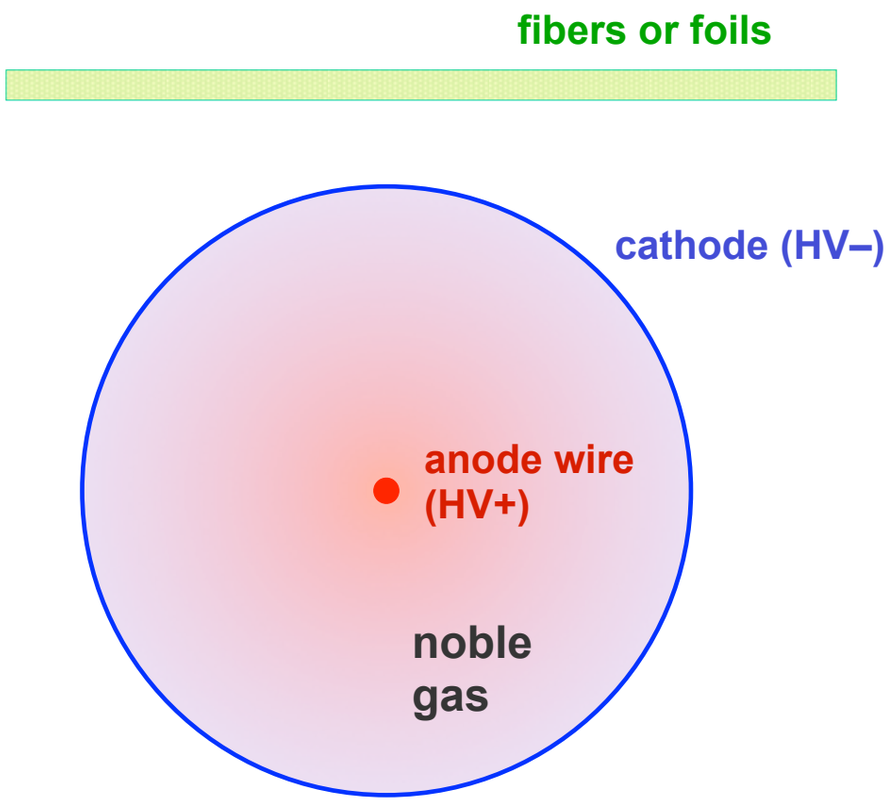

Combining Tracking with PID: the ATLAS TRT

- *e*/π separation via transition radiation: polymer (PP) fibers/foils interleaved with drift tubes

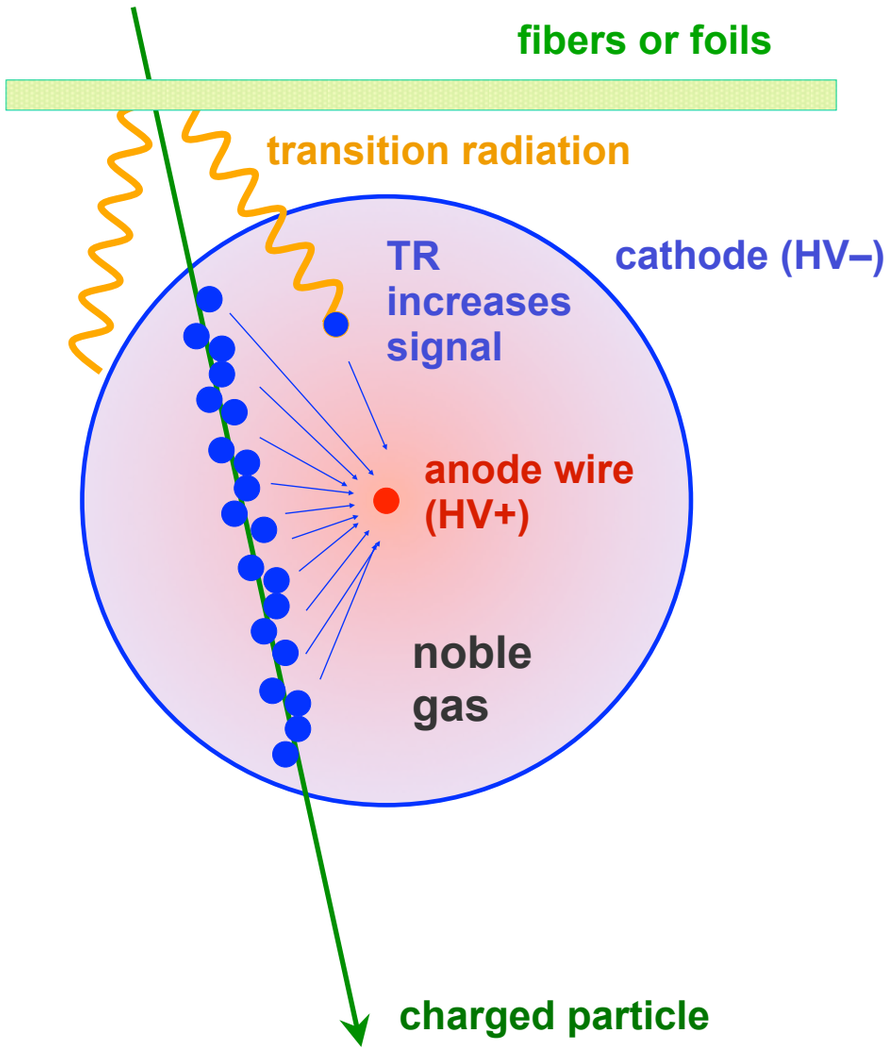

electrons radiate → higher signal
PID info by counting high-threshold hits

Combining Tracking with PID: the ATLAS TRT

- e/π separation via transition radiation: polymer (PP) fibers/foils interleaved with drift tubes

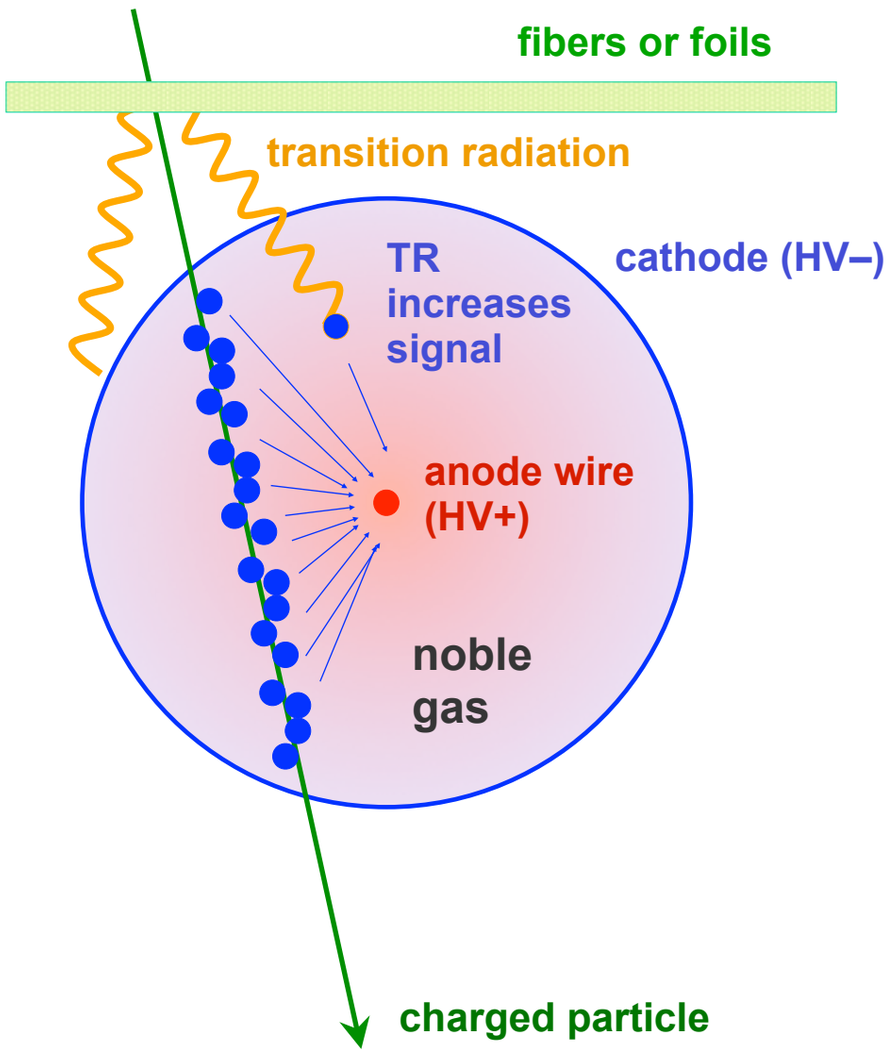

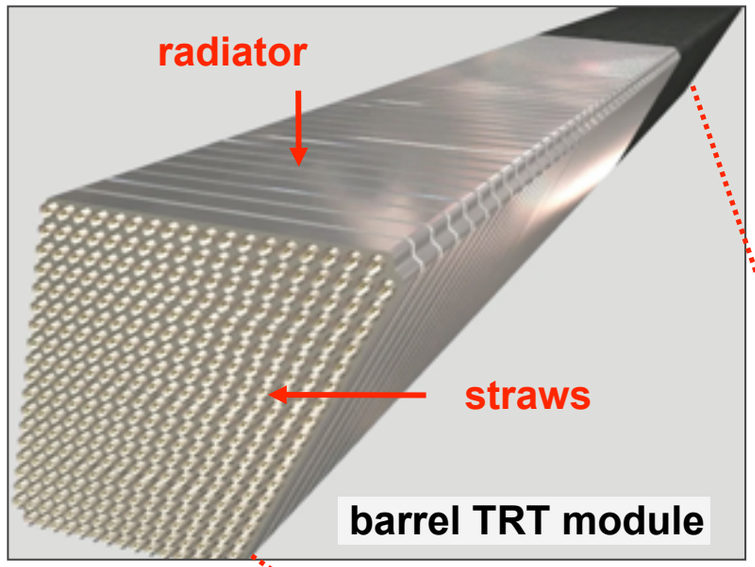

total: 370k straws

barrel ($|\eta| < 0.7$):
36 r-ϕ measurements / track
resolution ~130 μm / straw

14 end-cap wheels ($|\eta| < 2.1$):
40 or less z-ϕ points

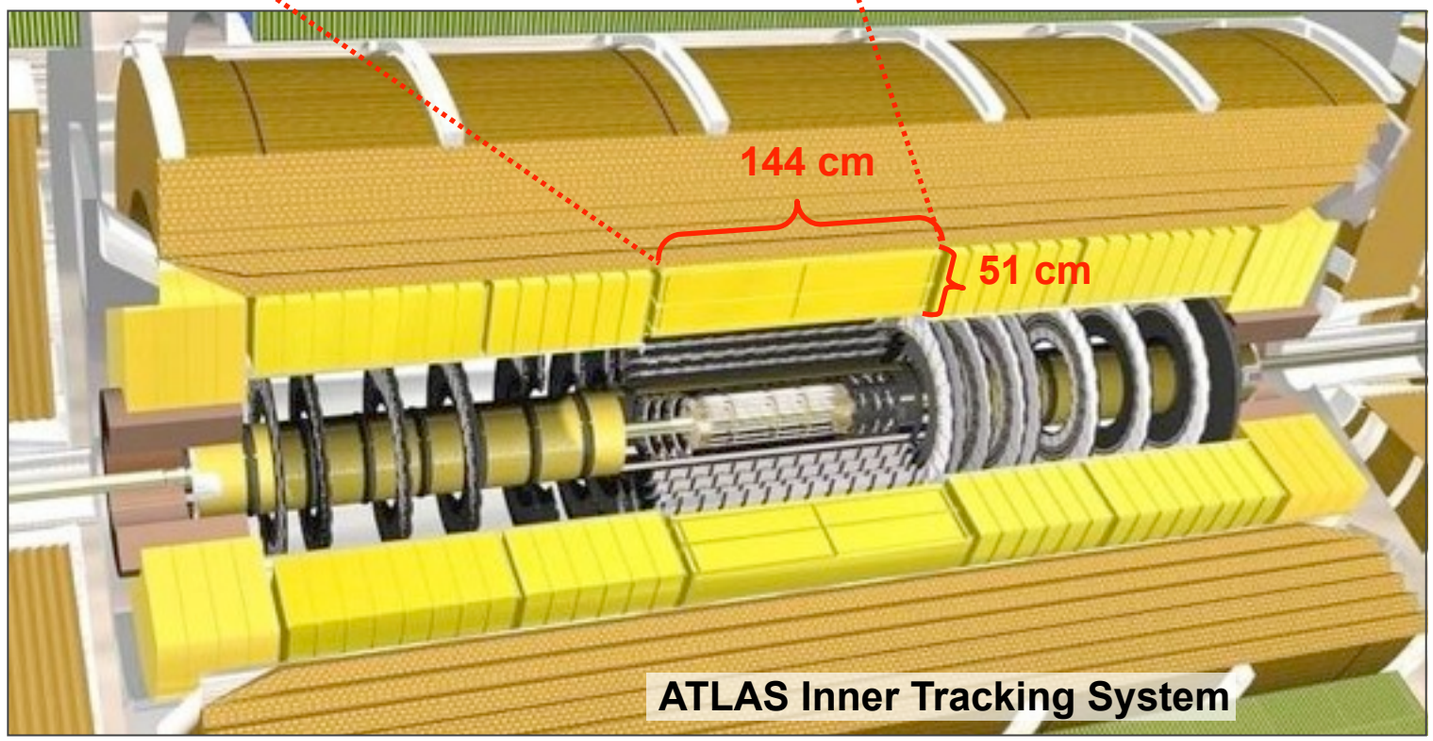

electrons radiate → higher signal
PID info by counting high-threshold hits

Time Projection Chambers

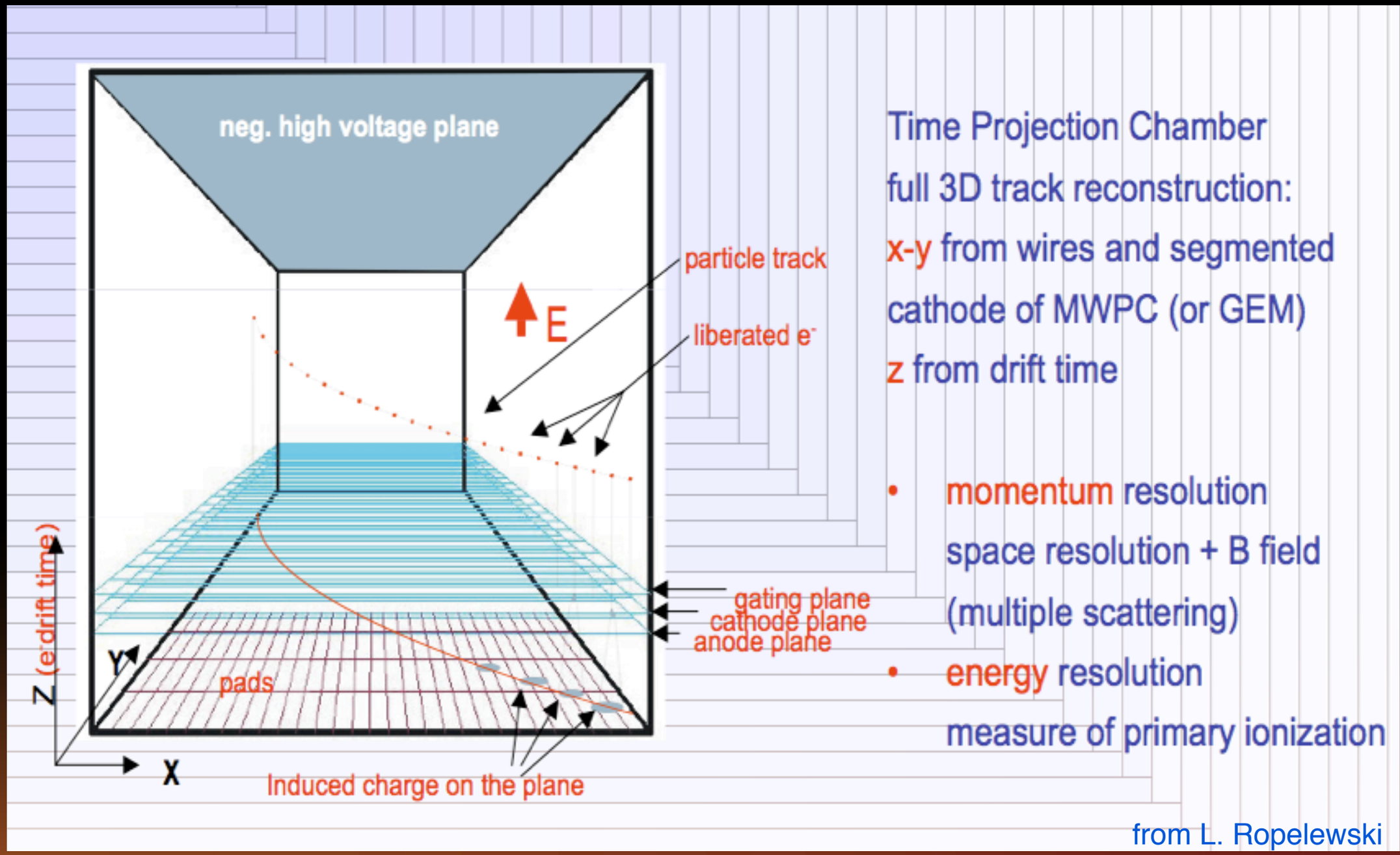

- developed by D. Nygren in the 70's.
- long drift times (≈ 40 μs), thus rate limitations and very good gas quality required

Most challenging TPC ever built

2x18 Inner Readout Chambers

2x18 Outer Readout Chambers

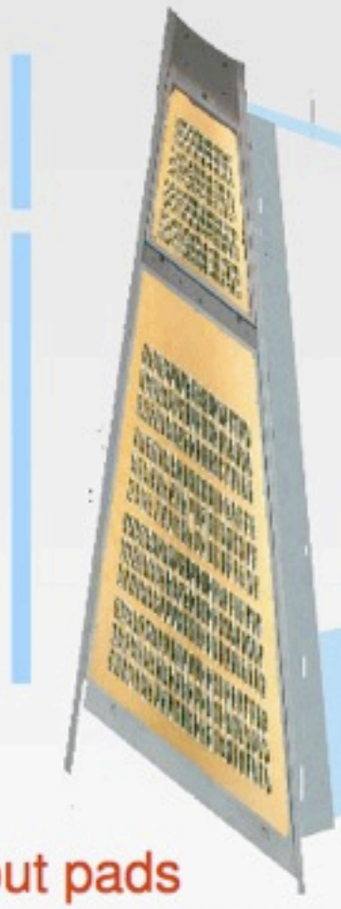

557568 readout pads

1000 samples in time direction

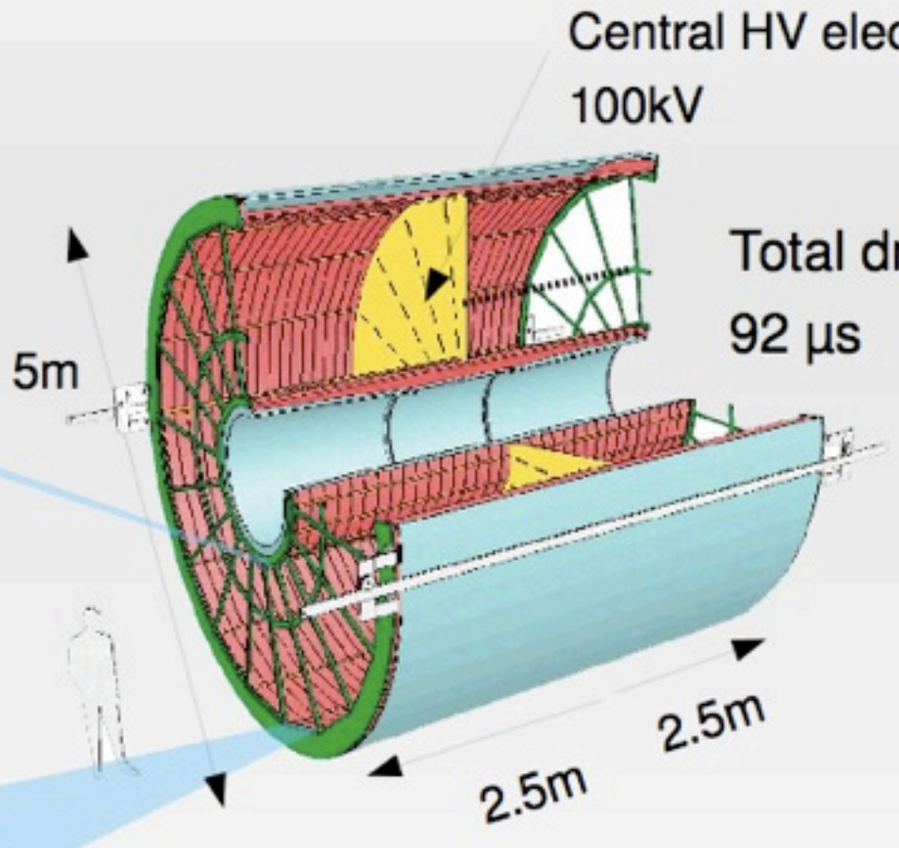

Gas:

- 90 m^3 of Ne-CO_2-N_2 (90 - 10 - 5)
- low diffusion (“cold gas”)
- drift velocity non saturated
  - temp. stability of 0.1K required

➡ ALICE data taking rate 1 kHz in pp

➡ few 100 Hz in Pb Pb

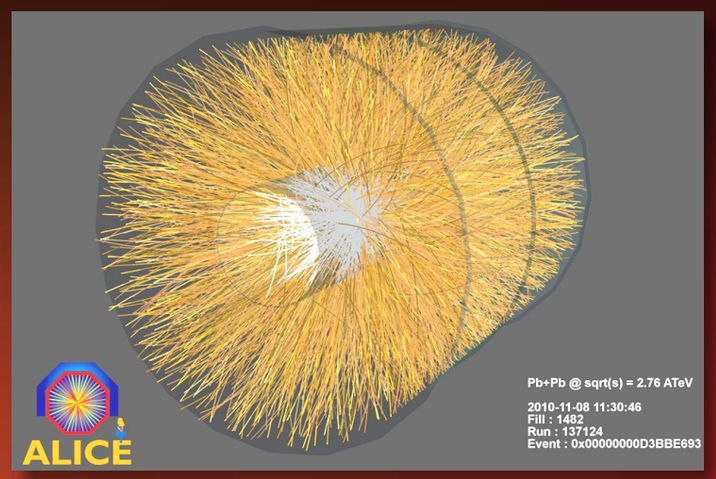

ALICE Tracking

➡ ITS : 6 layers
- 2 Pixels
- 2 silicon drift detectors
- 2 double sided strips

➡ Time Projection Chamber
- large volume gas detector with central electrode
- MWPC with cathode pad readout in end plates
- very good two-track resolution
- very low material in active region

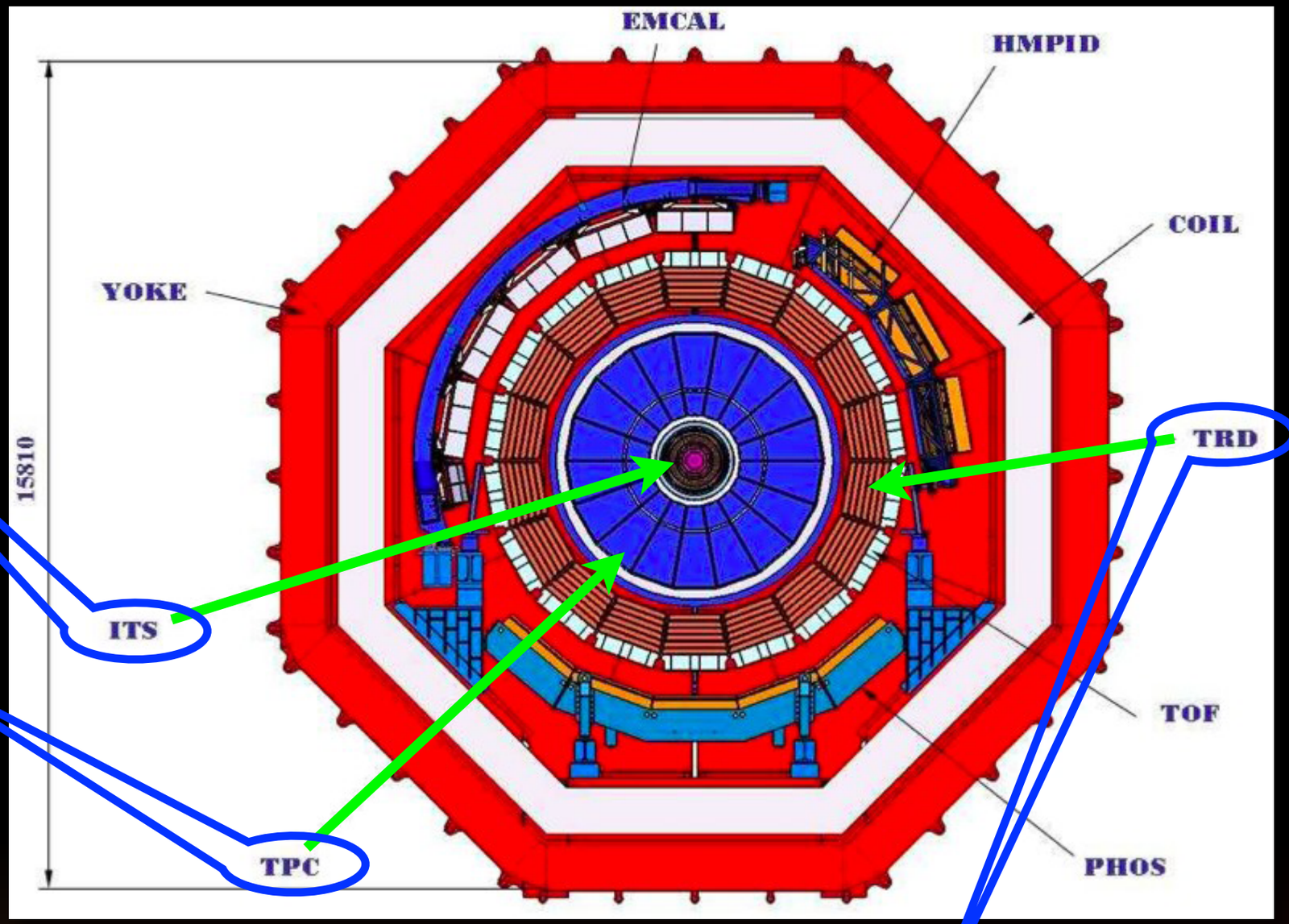

ITS: 3 different silicon detector technologies

Strip Drift Pixel

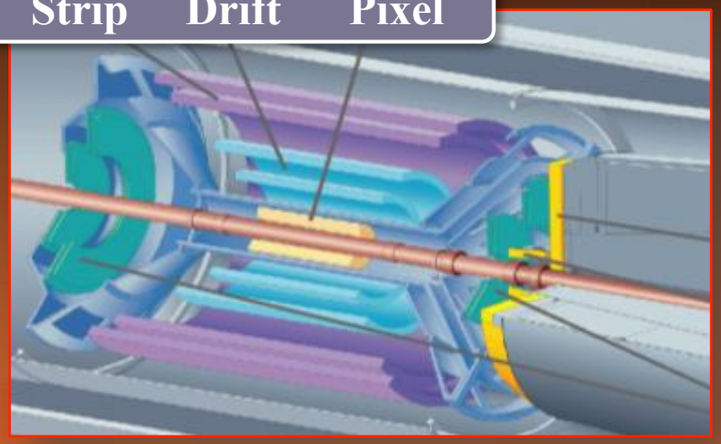

➡ Transition Radiation Detector
- electron ID, and improves momentum resolution
- outer radius 3.7m

➡ installed in L3 magnet
- lower B field (0.5 T) , larger R

Comparison of Barrel Tracker Layouts

P.Wells	ALICE	ATLAS	CMS
R inner	3.9 cm	5.0 cm	4.4 cm
R outer	3.7 m	1.1 m	1.1 m
Length	5 m	5.4 m	5.8 m
$\|\eta\|$ range	0.9	2.5	2.5
B field	0.5 T	2 T	4 T
Total X_0 near η=0	0.08 (ITS) + 0.035 (TPC) + 0.234 (TRD)	0.3	0.4
Power	6 kW (ITS)	70 kW	60 kW
rϕ resolution near outer radius	~ 800 μm TPC ~ 500 μm TRD	130 μm per TRT straw	35 μm per strip layer
p_T resolution at 1GeV and at 100 GeV	0.7% 3% (in pp)	1.3% 3.8%	0.7% 1.5%

- LHCb is a spectrometer designed for B-physics
  - ➡ p_T resolution is 0.35% at 1 GeV, 0.55% at 100 GeV for good mass resolution

Summary of Pixel Barrel Layouts

P.Wells	ALICE	ATLAS	CMS
Radii (mm)	39 – 76	50.5 – 88.5 – 122.5	44 – 73 – 102
Pixel size $r\phi$ x z (μm^2)	50 x 425	40 x 400	100 x 150
Thickness (μm)	200	250	285
Resolution $r\phi$ / z (μm)	12 / 100	10 / 115	~15-20
Channels (million)	9.8	80.4	66
Area (m^2)	0.2	1.8	1

- LHCb VELO
  - ➡ forward geometry strip detector with 42 stations along, inner radius of 7 mm
  - ➡ moves close to beam when conditions are stable

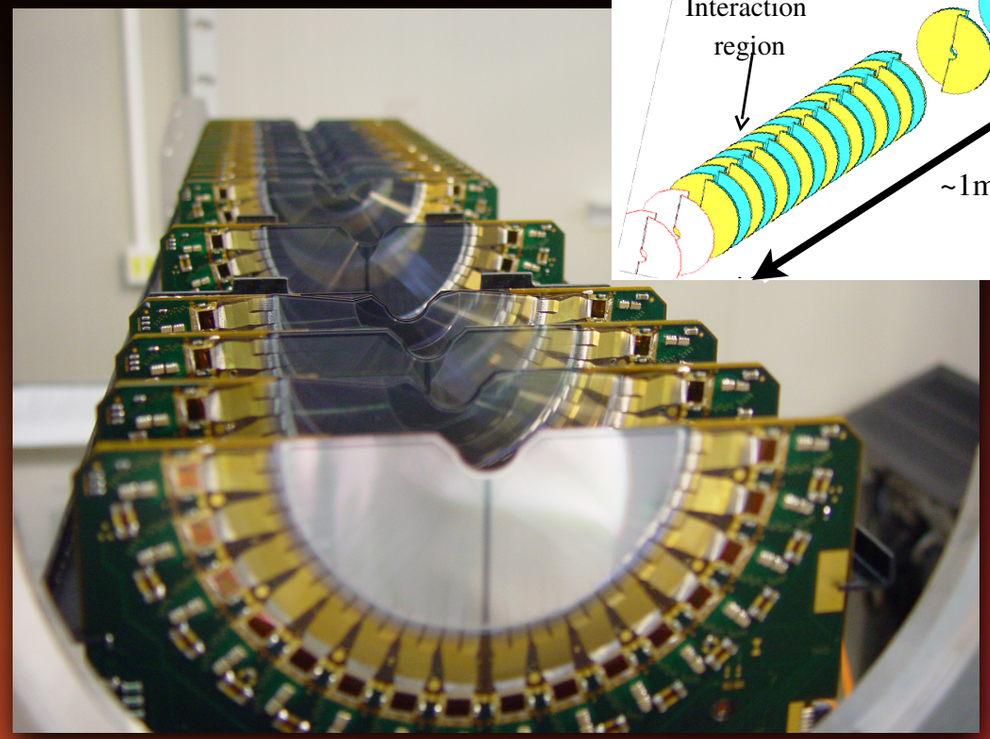

Summary of Pixel Barrel Layouts

P.Wells	ALICE	ATLAS	CMS
Radii (mm)	39 – 76	50.5 – 88.5 – 122.5	44 – 73 – 102
Pixel size $r\phi$ x z (μm^2)	50 x 425	40 x 400	100 x 150
Thickness (μm)	200	250	285
Resolution $r\phi$ / z (μm)	12 / 100	10 / 115	~15-20
Channels (million)	9.8	80.4	66
Area (m^2)	0.2	1.8	1

- LHCb VELO
  - ➡ forward geometry strip detector with 42 stations along, inner radius of 7 mm
  - ➡ moves close to beam when conditions are stable

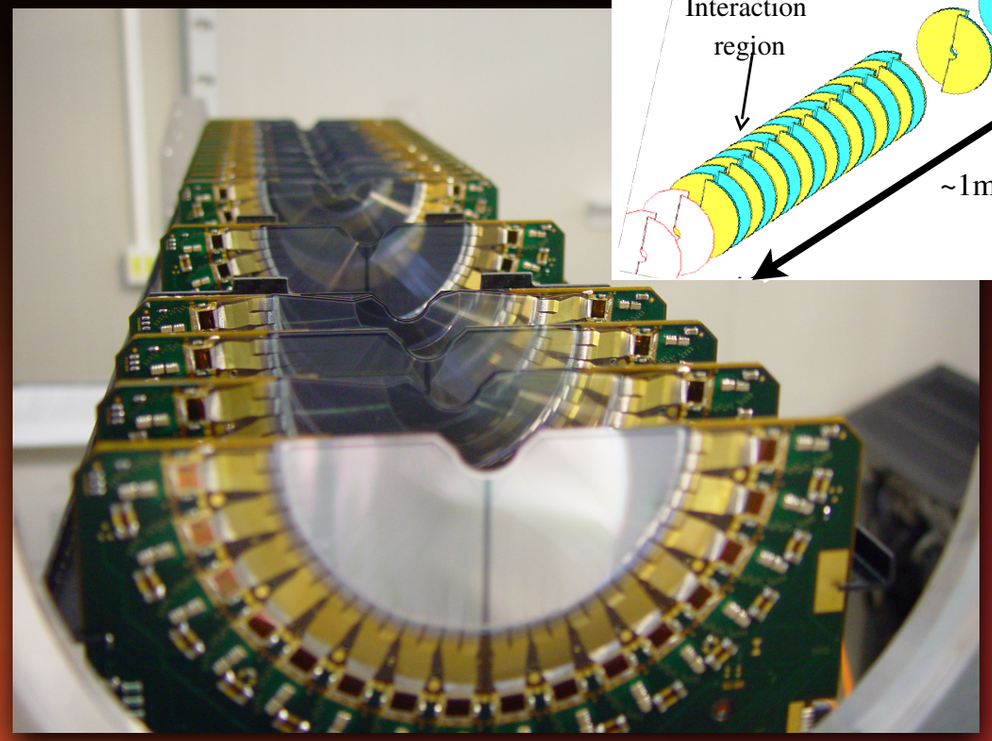

LHCb Tracking

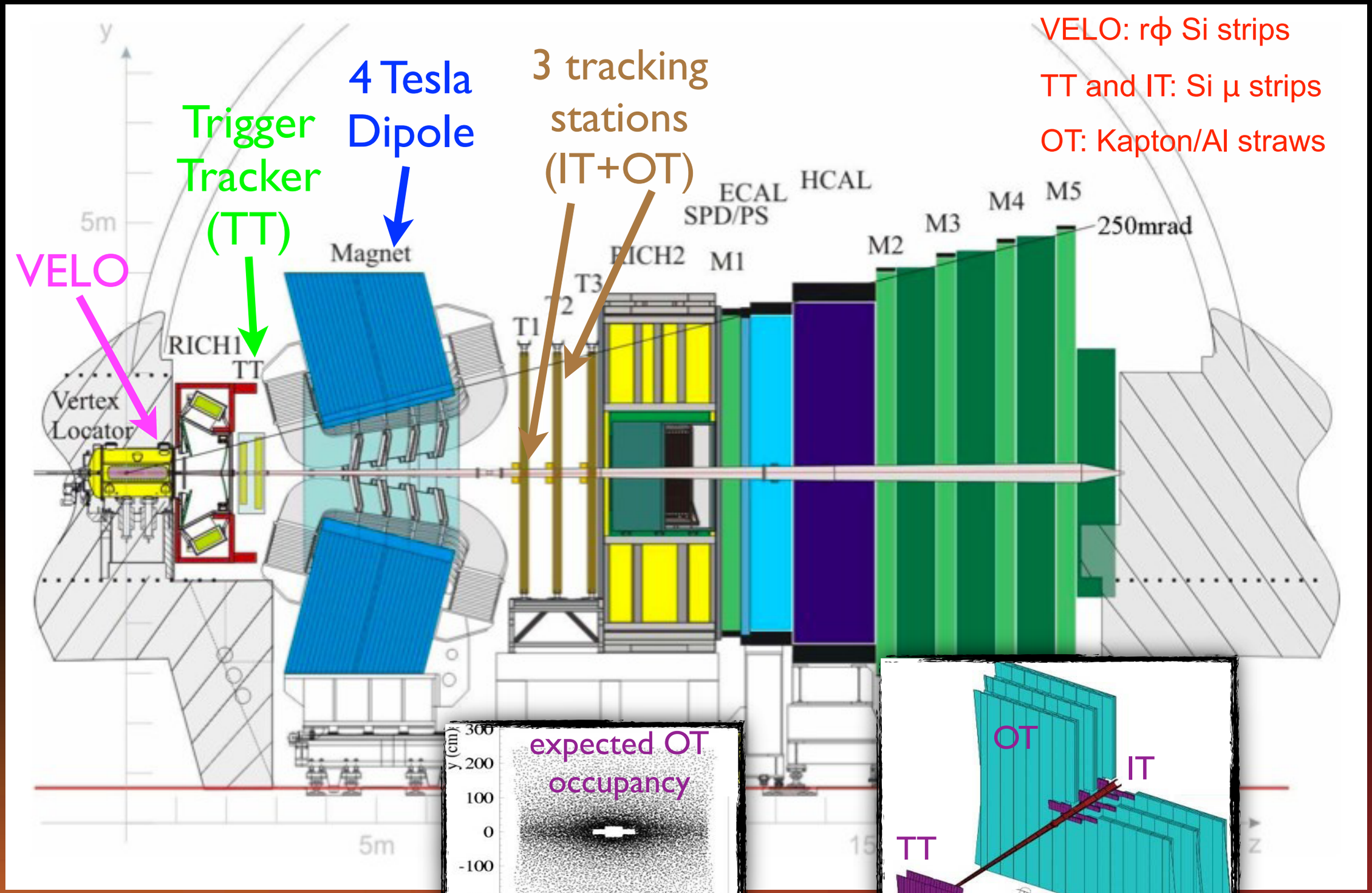

Let's Summarize

- discussed physics of particles in material
- in this lecture I discussed tracking detectors
  - ➡ main design choices and constraints
  - ➡ silicon and drift tube detectors
  - ➡ LHC tracking detector layouts
- next I will discuss track reconstruction